



1 **Millennial-scale variations of sedimentary oxygenation in the western**
2 **subtropical North Pacific and its links to the North Atlantic climate**

3

4 Jianjun Zou^{1,2}, Xuefa Shi^{1,2}, Aimei Zhu¹, Selvaraj Kandasamy³, Xun Gong⁴, Lester
5 Lembke-Jene⁴, Min-Te Chen⁵, Yonghua Wu^{1,2}, Shulan Ge^{1,2}, Yanguang Liu^{1,2}, Xinru
6 Xue¹, Gerrit Lohmann⁴, Ralf Tiedemann⁴

7 ¹Key Laboratory of Marine Sedimentology and Environmental Geology, First Institute
8 of Oceanography, MNR, Qingdao 266061, China

9 ²Laboratory for Marine Geology, Qingdao National Laboratory for Marine Science
10 and Technology, Qingdao, 266061, China

11 ³Department of Geological Oceanography and State Key Laboratory of Marine
12 Environmental Science, Xiamen University, Xiamen 361102, China

13 ⁴Alfred-Wegener-Institut Helmholtz-Zentrum für Polar- und Meeresforschung,
14 Bussestr. 24, 27570 Bremerhaven, Germany

15 ⁵Institute of Applied Geosciences, National Taiwan Ocean University, Keelung 20224,
16 Taiwan

17

18 Corresponding authors:

19 Jianjun Zou (zoujianjun@fio.org.cn); Xuefa Shi (xfshi@fio.org.cn)

20

21 **Key Points**

22 1. History of sedimentary oxygenation processes at mid-depths in the western
23 subtropical North Pacific since the Last Glacial is reconstructed using sediment-bound
24 geochemical proxies.

25 2. Redox-sensitive proxies reveal millennial-scale variations in sedimentary
26 oxygenation that correlated closely to changes in the North Pacific Intermediate
27 Water.

28 3. A millennial-scale out-of-phase relationship between deglacial ventilation in the
29 western subtropical North Pacific and the formation of North Atlantic Deep Water is
30 suggested.



31 4. A larger CO₂ storage at mid-depths of the North Pacific corresponds to the
32 termination of atmospheric CO₂ rise during the Bölling-Alleröd interval.
33



34 **Abstract**

35 Lower glacial atmospheric CO₂ concentrations have been attributed to carbon
36 sequestration in deep oceans. However, potential roles of voluminous subtropical
37 North Pacific in modulating atmospheric CO₂ levels on millennial timescale are
38 poorly constrained. Further, an increase in respired CO₂ concentration in the glacial
39 deep ocean due to biological pump generally is coeval with less oxygenation in the
40 subsurface layer. This link thus offers a chance to visit oceanic ventilation and the
41 coeval export productivity based on redox-controlled sedimentary geochemical
42 parameters. Here we investigate a suite of sediment geochemical proxies to
43 understand the sedimentary oxygenation variations in the subtropical North Pacific
44 (core CSH1) over the last 50 thousand years (ka). Our results suggest that sedimentary
45 oxygenation at mid-depths of the subtropical North Pacific intensifies during the
46 episodes of late glacial (50-25 ka), Last Glacial Maximum (LGM) and also the
47 interval after 8.5 ka, especially pronounced for the North Atlantic millennial-scale
48 abrupt cold events of the Younger Dryas, Heinrich Stadial (HS) 1 and 2. On the other
49 hand, oxygen-depleted seawater is found during the Bölling - Alleröd (B/A) and
50 Preboreal. Our findings of enhanced sedimentary oxygenation in the subtropical North
51 Pacific is aligned with intensified formation of North Pacific Intermediate Water
52 (NPIW) during cold spells, while the ameliorated sedimentary oxygenation seems to
53 be linked with the intensified Kuroshio Current since 8.5 ka. In our results,
54 diminished sedimentary oxygenation during the B/A indicates an enhanced CO₂
55 sequestration at mid-depth waters, along with slight increase in atmospheric CO₂
56 concentration. Mechanistically, we speculate that these millennial-scale changes were
57 linked to the strength of North Atlantic Deep Water, leading to intensification of
58 NPIW formation and enhanced abyss flushing during deglacial cold and warm
59 intervals, respectively. Enhanced formation of NPIW seem to be driven by the
60 perturbation of sea ice formation and sea surface salinity oscillation in high latitude
61 North Pacific through atmospheric and oceanic teleconnection. During the B/A,
62 decreased sedimentary oxygenation likely resulted from an upward penetration of
63 aged deep water into the intermediate-depth in the North Pacific, corresponding to a



64 resumption of Atlantic Meridional Overturning Circulation.

65 **Keywords:** sedimentary oxygenation; millennial timescale; North Pacific

66 Intermediate Water; Atlantic Meridional Overturning Circulation; subtropical North

67 Pacific

68



69 1. Introduction

70 The sluggish ocean ventilation depletes dissolved oxygen in the sediment-water
71 interface and facilitates the storage of respired carbon, which in turn plays a role in
72 regulating sedimentary oxygen, potentially linking to atmospheric CO₂ changes on
73 orbital and millennial timescales (Jaccard and Galbraith, 2012; Lu et al., 2016;
74 Sigman and Boyle, 2000). The reconstruction of past sedimentary oxygenation is
75 therefore crucial for understanding changes in export productivity and the renewal
76 rate of deep ocean circulation (Nameroff et al., 2004). Previous studies from
77 high-latitude North Pacific margins and subarctic Pacific have identified drastic
78 variations in export productivity and marine oxygen levels at glacial-interglacial
79 timescales using diverse proxies such as trace elements (Cartapanis et al., 2011;
80 Chang et al., 2014; Jaccard et al., 2009; Zou et al., 2012), benthic foraminiferal
81 assemblages (Ohkushi et al., 2016; Ohkushi et al., 2013; Shibahara et al., 2007) and
82 nitrogen isotopic composition ($\delta^{15}\text{N}$) of organic matter (Chang et al., 2014; Galbraith
83 et al., 2004; Riethdorf et al., 2016) in cored sediments. These studies further
84 suggested that both North Pacific Intermediate Water (NPIW) and export of organic
85 carbon regulate the sedimentary oxygenation variation during the last glaciation and
86 Holocene in the northeast North Pacific. By contrast, little information exists on
87 millennial-scale oxygenation changes to date in the western subtropical North Pacific.

88 The modern NPIW is mainly sourced from the NW Pacific marginal seas
89 (Shcherbina et al., 2003; Talley, 1993; You et al., 2000), and then it spreads into
90 subtropical North Pacific at intermediate depths of 300 to 800 m (Talley, 1993). The
91 pathway and circulation of NPIW have been identified by You (2003), who suggested
92 that cabbeling is the principle mechanism responsible for transforming subpolar
93 source waters into subtropical NPIW along the subarctic-tropical frontal zone. More
94 specifically, You et al. (2003) argued that a lower subpolar input of about 2Sv is
95 sufficient for subtropical ventilation. Benthic foraminiferal $\delta^{13}\text{C}$ data from the North
96 Pacific suggested enhanced ventilation at water depths of < 2000 m during the last
97 glacial period (Keigwin, 1998; Matsumoto et al., 2002). Furthermore, on the basis of
98 both radiocarbon data and modeling results, Okazaki et al. (2010) provided further



99 insight into the formation of deep water in the North Pacific during early deglaciation.
100 Enhanced NPIW penetration is further explored using numerical model simulations
101 (Chikamoto et al., 2012; Gong et al., 2019; Okazaki et al., 2010). The downstream
102 effects of intensified GNPIW can be seen in the record of $\delta^{13}\text{C}$ of *Cibicides*
103 *wuellerstorfi* in core PN-3 from the middle Okinawa Trough (OT), whereas lower
104 deglacial $\delta^{13}\text{C}$ values were attributed to enhanced OC accumulation rates due to
105 higher surface productivity by Wahyudi and Minagawa (1997).

106 The Okinawa Trough is separated from the Philippine Sea by the Ryukyu Islands
107 and is an important channel of the northern extension of the Kuroshio in the western
108 subtropical North Pacific (Figure 1). Surface hydrographic characteristics of the OT
109 over glacial-interglacial cycles are largely influenced by the Kuroshio and East China
110 Sea Coastal Water (Shi et al., 2014); the latter is related to the strength of summer
111 East Asian monsoon (EAM) sourced from the western tropical Pacific. Modern
112 physical oceanographic investigations showed that intermediate waters in the OT are
113 mainly derived from horizontal advection and mixture of NPIW and South China Sea
114 Intermediate Water (Nakamura et al., 2013). These waters intrude into the OT through
115 two ways (Nakamura et al., 2013): (i) deeper part of the Kuroshio enters the OT
116 through the channel east of Taiwan (sill depth 775 m) and (ii) through the Kerama
117 Gap (sill depth 1100 m). In the northern OT, the occupied subsurface water mainly
118 flows through the Kerama Gap through horizontal advection from the Philippine Sea
119 (Nakamura et al., 2013). Recently, Nishina et al. (2016) found that an overflow
120 through the Kerama Gap controls the modern deep-water ventilation in the southern
121 OT.

122 Both surface hydrography and deep ventilation in the OT varied greatly since the
123 last glaciation. During the last glacials, the mainstream of the Kuroshio likely
124 migrated to the east of the Ryukyu Islands or and also became weaker due to lower
125 sea levels (Shi et al., 2014; Ujiie and Ujiie, 1999; Ujiie et al., 2003) and the
126 hypothetical emergence of a Ryukyu-Taiwan land bridge (Ujiie and Ujiie, 1999). In a
127 recent study, based on the Mg/Ca-derived temperatures in surface and thermocline
128 waters and planktic foraminiferal indicators of water masses from two sediment cores



129 located in the northern and southern OT, Ujiie et al. (2016) further argued that the
130 hydrological conditions of North Pacific Subtropical Gyre since MIS 7 is modulated
131 by the interaction between the Kuroshio and the NPIW. Besides the Kuroshio, the
132 flux of East Asian rivers to the East China Sea (ECS), which is related to the summer
133 EAM and the sea level oscillation coupled with topography are also regulating the
134 surface hydrography in the Okinawa Trough (Chang et al., 2009; Kubota et al., 2010;
135 Sun et al., 2005; Yu et al., 2009).

136 Based on benthic foraminiferal assemblages, previous studies have implied a
137 reduced oxygenation in deep waters of the middle and southern OT during the last
138 deglacial period (Jian et al., 1996; Li et al., 2005), but a strong ventilation during the
139 Last Glacial Maximum (LGM) and the Holocene (Jian et al., 1996; Kao et al., 2005).
140 High sedimentary $\delta^{15}\text{N}$ values, an indicator of increased denitrification in the
141 subsurface water column, also occurred during the late deglaciation in the middle
142 OT (Kao et al., 2008). Inconsistent with these results, Dou et al. (2015) suggested an
143 oxic depositional environment during the last deglaciation in the southern OT based
144 on weak positive cerium anomalies. Furthermore, Kao et al. (2006) concluded a
145 reduced ventilation of deepwater in the OT during the LGM due to the reduction of
146 KC inflow using a 3-D ocean model. Yet, the patterns and reasons that caused
147 sedimentary oxygenation in the OT thus remain unclear.

148 **2. Paleo-redox proxies**

149 Sedimentary redox condition is the balance between the rate of oxygen supply
150 from the overlying bottom water and the rate of oxygen removal from pore water
151 (Jaccard et al., 2016), processes that are closely related to the advection of submarine
152 ocean circulation and organic matter respiration, respectively. Contrasting
153 geochemical behaviors of redox-sensitive trace metals (Mn, Mo, U, etc.) have been
154 extensively used to reconstruct bottom water and sedimentary oxygen changes (Algeo,
155 2004; Algeo and Lyons, 2006; Crusius et al., 1996; Dean et al., 1997; Tribovillard et
156 al., 2006; Zou et al., 2012), as their concentrations respond to redox condition of the
157 depositional environment (Morford and Emerson, 1999).

158 In general, enrichment of Mn with higher speciation states (Mn (III) and Mn (IV))



159 in the form of Mn-oxide coatings is observed in marine sediments, when oxic
160 condition prevails into great sediment depths as a result of low organic matter
161 degradation rates and well-ventilated bottom water (Burdige, 1993). In reducing
162 conditions, Mn is released as dissolved Mn (II) species into the pore water and thus its
163 concentration is usually low in suboxic (O_2 and HS^- absent) and anoxic (HS^- present)
164 sediments. In addition, when Mn enrichment occurs in oxic sediments as solid phase
165 Mn oxyhydroxides, it may lead to co-precipitation of other elements, such as Mo
166 (Nameroff et al., 2002).

167 The elements Mo and U behave conservatively in oxygenated seawater, but are
168 preferentially enriched in oxygen-depleted water. However, these two trace metals
169 behave differently in several ways. Molybdenum can be enriched in both oxic
170 sediments, such as the near surface manganese-rich horizons in continental margin
171 environments (Shimmield and Price, 1986) and in anoxic sediments (Nameroff et al.,
172 2002). Under anoxic conditions, Mo can be reduced either from the +6 oxidation state
173 to insoluble MoS_2 , though this process is known to occur only under extremely
174 reducing conditions, such as hydrothermal and/or diagenesis (Dahl et al., 2010; Helz
175 et al., 1996) or be converted to particle-reactive thiomolybdates (Vorlicek and Helz,
176 2002). Zheng et al. (2000) suggested two critical thresholds for Mo scavenging from
177 seawater: $0.1\mu M$ hydrogen sulfide (H_2S) for Fe-S-Mo co-precipitation and $100\mu M$
178 H_2S for Mo scavenging as Mo-S or as particle-bound Mo without Fe. Although
179 Crusius et al. (1996) noted insignificant enrichment of sedimentary Mo under suboxic
180 conditions, Scott et al. (2008) argued that burial flux of Mo is not so low in suboxic
181 environments. Excess concentration of Mo (Mo_{excess}) in sediments thus suggests the
182 accumulation of sediments either in anoxic (H_2S occurrence) or well oxygenated
183 conditions (if Mo_{excess} is in association with Mn-oxides).

184 In general, U is enriched in anoxic sediments ($>1\mu M H_2S$), but not in oxic
185 sediments ($>10\mu M O_2$) (Nameroff et al., 2002). Accumulation of U depends on the
186 content of reactive organic matter (Sundby et al., 2004) and U precipitates as uraninite
187 (UO_2) during the conversion of Fe (III) to Fe (II) in suboxic conditions (Morford and
188 Emerson, 1999; Zheng et al., 2002). One of the primary removal mechanisms for U



189 from the ocean is via diffusion across the sediment-water interface of reducing
190 sediments (Klinkhammer and Palmer, 1991). Under suboxic conditions, soluble U (VI)
191 is reduced to insoluble U (IV), but free sulfide is not required for U
192 precipitation (McManus et al., 2005). Jaccard et al. (2009) suggested that the presence
193 of excess concentration of U (U_{excess}) in the absence of Mo enrichment is indicative of
194 a suboxic, but not sulfidic condition, within the diffusional range of the
195 sediment-water interface. The felsic volcanic is also a primary source of uranium
196 (Maithani and Srinivasan, 2011). Therefore, the potential input of uranium from active
197 volcanic sources around the northwestern Pacific to the adjacent sediments should not
198 be neglected.

199 In this study, we investigate a suite of redox-sensitive elements and the ratio of
200 Mo/Mn along with productivity proxies from a sediment core retrieved from the
201 northern OT to reconstruct the sedimentary oxygenation in the western subtropical
202 North Pacific over the last 50ka. Based on that, we propose that multiple factors, such
203 as NPIW ventilation, the strength of the Kuroshio Current and export productivity,
204 control the bottom sedimentary oxygenation in the OT on millennial time scales since
205 the last glacial.

206 **3. Oceanographic setting**

207 The OT resulted from the collision of the Philippine and Eurasian plates and
208 initially opened at the middle Miocene (Sibuet et al., 1987). Since that time, the OT
209 has been a depositional center in the ECS and receives large sediment supplies from
210 nearby rivers (Chang et al., 2009). At present, water depth in the axial part of the OT
211 deepens from 500 m in the north to ~2700 m in the south.

212 Surface hydrographic characteristics of the OT are mainly controlled by the
213 warmer, more saline Kuroshio water and cooler, less saline Changjiang Diluted Water,
214 and the modern flow-path of the former is influenced by the bathymetry of the OT
215 (Figure 1a). The Kuroshio Current originates from the North Equatorial Current and
216 flows into the ECS from the Philippine Sea through the Suao-Yonaguni Depression.
217 In the northern OT, Tsushima Warm Current (TWC), a branch of the Kuroshio, flows
218 into the Japan Sea through the shallow Tsushima Strait. Volume transport of the



219 Kuroshio varies seasonally due to the influence of the EAM with a maximum of 24
220 Sv ($1 \text{ Sv} = 10^6 \text{ m}^3/\text{s}$) in summer and a minimum of 20 Sv in autumn across the east of
221 Taiwan (Qu and Lukas, 2003).

222 Figures 2a and b show the lower sea surface salinity (SSS) zone in summer in the
223 ECS migrates toward the east of OT, indicating enhanced impact of the Changjiang
224 discharge associated with summer EAM. The mean annual discharge of the
225 Changjiang is 0.028 Sv and ~80% of its total discharge is supplied to the ECS
226 (Ichikawa and Beardsley, 2002). In situ observational data of surface hydrography
227 along the ship track from Taiwan Strait to Korea Strait and around the entrance of the
228 Tsushima Strait in the northern part of the ECS show a lower SSS in summer and a
229 negative correlation between the Changjiang discharge and SSS in July (Delcroix and
230 Murtugudde, 2002). Lower SSS in summer than that in winter suggests stronger
231 effects of summer EAM on surface hydrography over the Kuroshio Current (Sun et al.,
232 2005). Consistently, previous studies from the Okinawa Trough reported such close
233 relationship between summer EAM and SSS back to the late Pleistocene (Chang et al.,
234 2009; Clemens et al., 2018; Kubota et al., 2010; Sun et al., 2005).

235 Despite the effects of EAM and the Kuroshio, evidence of geochemical tracers
236 (temperature, salinity, oxygen, nutrients and radiocarbon- $\Delta^{14}\text{C}$) collected during the
237 World Ocean Circulation Experiment (WOCE) Expeditions in the Pacific (transects
238 P24 and P03) favors the presence of low saline, nutrient-enriched intermediate and
239 deep waters (Talley, 2007). Dissolved oxygen content is $<100 \mu\text{M}$ at water depths of
240 below 600 m in the OT along WOCE transects PC03 and PC24 (Talley, 2007).
241 Modern oceanographic observations at the Kerama Gap reveal that upwelling in the
242 OT is associated with the inflow of NPIW and studies using box model predicted that
243 overflow through the Kerama Gap is responsible for upwelling ($3.8\text{--}7.6 \times 10^{-6} \text{ m s}^{-1}$)
244 (Nakamura et al., 2013; Nishina et al., 2016).

245 **4. Materials and methods**

246 **4.1. Chronostratigraphy of core CSH1**

247 A 17.3 m long sediment core CSH1 ($31^\circ 13.7' \text{ N}$, $128^\circ 43.4' \text{ E}$; water depth: 703
248 m) was collected from the northern OT, close to the main stream of TWC (Figure 1b)



249 and within the depth of NPIW (Figure 1c) using a piston corer during
250 *Xiangyanghong09* Cruise in 1998. This location is thus enabling us to reconstruct
251 millennial changes in the properties of TWC and NPIW. The expedition was carried
252 out by the First Institute of Oceanography, Ministry of Natural Resources of China.
253 Core CSH1 mainly consists of clayey silt and silt with occurrence of plant debris at
254 some depth intervals (Ge et al., 2007) (Figure 3a). In addition, three layers of volcanic
255 ash were observed at depths of 74–106 cm, 782–794 cm, 1570–1602 cm and these
256 three intervals can be correlated with well-known ash layers, Kikai-Akahoya (K-Ah;
257 7.3 ka), Aira-Tanzawa (AT; 29.24 ka) and Aso-4 (roughly around MIS 5a) (Machida,
258 1999), respectively. The core was split and sub-sampled at every 4 cm interval and
259 then stored in China Ocean Sample Repository at 4 °C until analysis.

260 Previously, some paleoceanographic studies have been conducted and a set of
261 data have been investigated for core CSH1, including the contents of planktic
262 foraminifers as well as their carbon ($\delta^{13}\text{C}$) and oxygen isotope ($\delta^{18}\text{O}$) compositions
263 (Shi et al., 2014), pollen (Chen et al., 2006), paleomagnetism (Ge et al., 2007) and
264 CaCO_3 (Wu et al., 2004). An age model for this core has been constructed by using
265 ten Accelerator Mass Spectrometry (AMS) ^{14}C dates and six oxygen isotope ($\delta^{18}\text{O}$)
266 age control points. The whole 17.3 m core contains *ca.* 88 ka-long record of
267 continuous sedimentation (Shi et al., 2014).

268 It is noteworthy that previous age control points with constant radiocarbon
269 reservoir throughout core CSH1 are used to reveal orbital-scale Kuroshio variations
270 (Shi et al., 2014), but insufficient to investigate millennial-scale climatic events. On
271 the basis of original age model, a higher abundance of *Neogloboquadrina*
272 *pachyderma (dextral)* that occurred during warmer intervals, such as the B/A, has
273 been challenging to explain reasonably. On the other hand, paired measurements of
274 $^{14}\text{C}/^{12}\text{C}$ and ^{230}Th ages from Hulu Cave stalagmites suggest magnetic field change has
275 greatly contributed to high atmospheric $^{14}\text{C}/^{12}\text{C}$ values at HS4 and the YD (Cheng et
276 al., 2018). Thus a constant reservoir age assumed when calibrating foraminiferal
277 radiocarbon dates using CALIB 6 software and the Marine13 calibration dataset
278 (Reimer et al., 2013) for Core CSH1 may cause large chronological uncertainties.



279 Here, we therefore recalibrated the radiocarbon dates using CALIB 7.04 software
280 with Marine 13 calibration dataset (Reimer et al., 2013). Moreover, on the basis of
281 significant correlation between planktic foraminiferal $\delta^{18}\text{O}$ and Chinese stalagmite
282 $\delta^{18}\text{O}$ (Cheng et al., 2016), a proxy of summer EAM related to SSS of ECS, we
283 re-established the age model for core CSH1 (Figures 3b-d). Overall, the new
284 chronological framework is similar to the one previously reported by Shi et al. (2014),
285 but with more dates. In order to compare with published results associated with
286 ventilation changes in the North Pacific, here we mainly report the history of
287 sedimentary oxygenation in the northern OT since the last glacial. Linear
288 sedimentation rate varied between 10 and 60 cm/ka. The age control points were
289 shown in Table 2.

290 **4.2. Chemical analyses**

291 Sediment subsamples for geochemical analyses were freeze-dried and ground to
292 a fine powder with an agate mortar and pestle. Based on the age model, 85
293 subsamples from core CSH1 with time resolution of about 200 years (4 cm interval)
294 were selected for detailed geochemical analyses of major and minor elements and
295 total contents of carbon (TC), organic carbon (TOC) and nitrogen (TN). The
296 pretreatment of sediment and other analytical methods have been reported elsewhere
297 (Zou et al., 2012)

298 TC and TN were determined with an elemental analyzer (EA; Vario EL III,
299 Elementar Analysen systeme GmbH) in the Key Laboratory of Marine Sediment and
300 Environment Geology, First Institute of Oceanography, Ministry of Natural Resources
301 of China, Qingdao. Carbonate was removed from sediments by adding 1M HCl to the
302 homogenized sediments for total organic carbon (TOC) analysis using the same
303 equipment. The content of calcium carbonate (CaCO_3) was calculated using the
304 equation:

$$305 \quad \text{CaCO}_3 = (\text{TC} - \text{TOC}) \times 8.33$$

306 where 8.33 is the ratio between the molecular weight of carbonate and the atomic
307 weight of carbon. National reference material (GSD-9), blank sample and replicated
308 samples were used to control the analytical process. The relative standard deviation of



309 the GSD-9 for TC, TN and TOC is $\leq 3.4\%$.

310 About 0.5 g of sediment powder was digested in double distilled HF:HNO₃ (3:1),
311 followed by concentrated HClO₄, and then re-dissolved in 5% HNO₃. Selected major
312 and minor elements such as aluminum (Al) and manganese (Mn) were determined by
313 inductively coupled plasma optical emission spectroscopy (ICP-OES; Thermo
314 Scientific iCAP 6000, Thermo Fisher Scientific), as detailed elsewhere (Zou et al.,
315 2012). In addition, Mo and U were analyzed with inductively coupled plasma mass
316 spectrometry (ICP-MS; Thermo Scientific XSERIES 2, Thermo Fisher Scientific), as
317 described in Zou et al. (2012). Precision for most elements in the reference material
318 GSD-9 is $\leq 5\%$ relative standard deviation. The excess fractions of U and Mo were
319 estimated by normalization to Al:

320 Excess fraction = $\frac{\text{total}_{\text{element}} - (\text{element}/\text{Al}_{\text{average shale}} \times \text{Al})}{\text{Al}_{\text{average shale}}}$, with $\text{U}/\text{Al}_{\text{average shale}} =$
321 0.307×10^{-6} and $\text{Mo}/\text{Al}_{\text{average shale}} = 0.295 \times 10^{-6}$ (Li and Schoonmaker, 2014).

322 In addition, given the different geochemical behaviors of Mn and Mo and
323 co-precipitation and adsorption processes associated with the redox cycling of Mn, we
324 calculated the ratio of Mo to Mn, given that higher Mo/Mn ratio indicates lower
325 oxygen content in the depositional environment and vice versa. In combination with
326 the concentration of excess uranium, we infer the history of sedimentary oxygenation
327 in the subtropical North Pacific since the last glaciation.

328 **5. Results**

329 **5.1. TOC, TN, and CaCO₃**

330 TN content shows a larger variation compared to TOC (Figure 4b), but it still
331 strongly correlates with TOC ($r = 0.74$, $p < 0.01$) throughout the entire core.
332 Concentration of TOC ranges from 0.5 to 2.1% and it shows higher values with stable
333 trends during the last glacial phase (MIS 3) (Figure 4c). Molar ratios of TOC/TN vary
334 around 10, with higher ratios at the transition into the LGM (Figure 4d),
335 corresponding to higher linear sedimentation rate (Figure 4a). The content of CaCO₃
336 varies from 8.8 to 35% (Figure 4e) and it mostly shows higher values with increasing
337 trends during the last deglaciation. Conversely, the content of CaCO₃ is low and
338 exhibits decreasing trends during late MIS 3 and the LGM (Figure 4e).



339 Both TOC and CaCO_3 are widely used as proxies for the reconstruction of past
340 export productivity (Rühlemann et al., 1999). Molar C/N ratios of >10 (Figure 4c)
341 suggest that terrigenous organic sources significantly contribute to the TOC
342 concentration in core CSH1. The TOC content therefore may be not a reliable proxy
343 for the reconstruction of surface water export productivity during times of the LGM
344 and late deglaciation, when maxima in C/N ratios co-occur with decoupled trends
345 between CaCO_3 and TOC concentrations. In addition, the negative correlation
346 coefficient ($r = -0.85$, $p < 0.01$) between Al and CaCO_3 in sediments throughout core
347 CSH1 confirms the biogenic origin of CaCO_3 against terrigenous Al (Figure 4f).
348 Moreover, a detailed comparison between CaCO_3 concentrations and the previously
349 published foraminiferal fragmentation ratio (Wu et al., 2004) clearly shows, apart
350 from a small portion within the LGM, no clear co-variation. This suggests that CaCO_3
351 changes are primarily driven by variations in carbonate primary production, and not
352 overprinted by secondary processes, such as carbonate dissolution through changes in
353 the lysocline depth. On the other hand, terrigenous dilution generally decreases the
354 content of CaCO_3 . The increasing trend of CaCO_3 associated with high sedimentation
355 rate (Figures 4a, e) indicates a substantial increase in export productivity during the
356 last deglacial interval. Thus, we can confidently use CaCO_3 content as productivity
357 proxy to a first order approximation.

358 **5.2. Redox-sensitive Elements**

359 Figure 4 shows time series of selected redox-sensitive elements (RSEs) and
360 proxies derived from them. Mn shows higher concentrations during the LGM and
361 HS1 (16–22.5ka) and middle-late Holocene, but lower concentrations during the last
362 deglacial and Preboreal periods (15.8–9.5ka) (Figure 4g). Generally, concentrations of
363 excess Mo and excess U (Figures 4j, l) show coherent patterns with those of Mo and
364 U (Figures 4i, k), but both are out-of-phase with Mn over the last glacial period
365 (Figure 4h). It should be noted that pronounced variations in U concentration since
366 8.5 ka is related to the occurrence of discrete volcanic materials. A negative
367 correlation between Mn and $\text{Mo}_{\text{excess}}$ during the last glaciation and the Holocene, and
368 the strong positive correlation between them during the LGM and HS1 (Figures 5a



369 and 5b) further corroborate the complicated geochemical behavior of Mn and Mo. A
370 strong positive correlation between Mo_{excess} and Mn (Figure 5b) seems to be attributed
371 to co-precipitation of Mo by Mn-oxyhydroxide under oxygenated conditions. Here,
372 we use Mo/Mn ratio, instead of excess Mo concentration to reconstruct variations in
373 sedimentary redox state. Overall, the Mo/Mn ratio shows similar downcore pattern to
374 that of Mo_{excess} with higher values during the last deglaciation, but lower values
375 during the LGM and HS1. A strong correlation between Mo/Mn ratio and excess U
376 concentration (Figure 5c) further corroborates the integrity of Mo/Mn as an indicator
377 of sedimentary oxygenation changes.

378 Rapidly decreasing Mo/Mn ratio indicates an oxygenated sedimentary
379 environment since ~8 ka (Figure 4h). Both higher Mo/Mn ratios and excess U
380 concentration, together with lower Mn concentrations suggest an oxygen-deficient
381 sedimentary environment during the late deglacial period (15.8–9.5 ka), whereas
382 lower values during the LGM, HS1 and HS2 indicate relatively better oxygenated
383 sedimentary condition. A decreasing trend in Mo/Mn ratio and excess U concentration
384 from 50 ka to 25 ka also suggest higher sedimentary oxygen levels.

385 **6. Discussion**

386 **6.1. Constraining paleoredox conditions in the Okinawa Trough**

387 In general, three different terms, hypoxia, suboxia and anoxia, are widely used to
388 describe the degree of oxygen depletion in the marine environment (Hofmann et al.,
389 2011). Generally, redox states in waters can be classified as oxic ($>89 \mu\text{mol/L O}_2$),
390 suboxic ($\sim 8.9\text{--}89 \mu\text{mol/LO}_2$), anoxic–nonsulfidic ($<89 \mu\text{mol/L O}_2$, $0 \mu\text{mol/L H}_2\text{S}$),
391 and anoxic–sulfidic or euxinic ($0 \text{ ml O}_2/\text{L}$, $>0 \mu\text{mol/L H}_2\text{S}$) (Savrda and Bottjer,
392 1991).

393 Proxies associated with RSEs, such as sedimentary Mo concentration (Lyons et
394 al., 2009; Scott et al., 2008) have been used to constrain the degree of oxygenation in
395 seawater. Algeo and Tribovillard (2009) proposed that open-ocean systems with
396 suboxic waters tend to yield U_{excess} enrichment relative to Mo_{excess} and to result in
397 sediment $(Mo/U)_{\text{excess}}$ ratio less than that of seawater (7.5–7.9). Under increasingly
398 reducing and occasionally sulfidic conditions, the accumulation of Mo_{excess} increase



399 relative to that of U_{excess} leading the $(\text{Mo}/U)_{\text{excess}}$ ratio either is equal to or exceeds
400 with that of seawater. Furthermore, Scott and Lyons (2012) suggested a non-euxinic
401 condition with the presence of sulfide in pore waters, when Mo concentrations range
402 from > 2 ppm, the crustal average to < 25 ppm, a threshold concentration for euxinic
403 condition. Given that the Okinawa Trough is located in weakly restricted basin
404 settings, we use these two above mentioned proxies to evaluate the degree of
405 oxygenation in sediments.

406 Both bulk Mo concentration (1.2-9.5 ppm) and excess (Mo/U) ratio (0.2-5.7) in
407 core CSH1 suggest that oxygen-depleted conditions may have prevailed in the deep
408 water of the northern OT over the last 50 ka. However, increased excess Mo
409 concentration with enhanced Mo/U ratio during the last termination (18-9 ka) indicate
410 a stronger reducing condition compared to the Holocene and the last glacial period,
411 though Mo concentration is less than 25 ppm, a threshold for euxinic deposition
412 proposed by Scott and Lyons (2012).

413 The relative abundance of benthic foraminiferal species that thrive in different
414 oxygen concentrations also have been widely used to reconstruct the variations in
415 bottom water ventilation, such as enhanced abundance of *Bulimina aculeata*,
416 *Uvigerina peregrina* and *Chilostomella oolina* found under oxygen-depleted
417 conditions in the central and southern OT during the last deglaciation (Jian et al., 1996;
418 Li et al., 2005). An oxygenated bottom water condition is also indicated by abundant
419 benthic foraminifera species *Cibicidoides hyalina* and *Globocassidulina subglobosa*
420 (Jian et al., 1996; Li et al., 2005) and high benthic $\delta^{13}\text{C}$ values (Wahyudi and
421 Minagawa, 1997) in cores E017 (water depth 1826 m), 225 (water depth 1575 m) and
422 PN-3 (water depth 1058 m) from the middle and southern OT (Figures 1 and 3)
423 during the postglacial period. The inferred ventilation pattern from benthic
424 foraminiferal assemblages is consistent with the one inferred from RSEs in this study
425 (Figure 4). Although we did not carry out benthic foraminiferal species analyses for
426 our core CSH1, it is reasonable to infer based on RSEs that the deepwater in the
427 northern OT was also in a prominent oxygen-poor condition during the late deglacial
428 interval. A clear link thus can be built between the ventilation of deep water and the



429 sedimentary oxygenation in the OT. In brief, our proxy records of RSEs in core CSH1
430 show oxygen-rich conditions during the last glaciation and middle and late Holocene
431 (since 8.5 ka) intervals, but oxygen-poor conditions during the late deglacial period.

432 **6.2. Causes for sedimentary oxygenation variations**

433 As discussed above, the pattern of RSEs in core CSH1 suggest that drastic
434 changes in sedimentary oxygenation occurred on orbital and millennial timescales
435 over the last glaciation in the Okinawa Trough. In general, four factors can regulate
436 the redox condition in the deep water column: (i) O₂ solubility, (ii) export productivity
437 and subsequent degradation of organic matter, (iii) vertical mixing, and (iv) lateral
438 provision of oxygen through intermediate and deeper water masses (Ivanochko and
439 Pedersen, 2004; Jaccard and Galbraith, 2012). In the OT, the oxygen deficiency
440 during the late deglacial period can be caused either by one and/or a combination of
441 more than one of these factors. In order to uncover the mechanisms responsible for
442 sedimentary oxygenation variations in the basin-wide OT, we compare our proxy
443 records of sedimentary oxygenation (U_{excess} concentration and Mo/Mn ratio) and
444 export productivity (CaCO₃) with benthic foraminifera δ¹³C, a proxy for water mass,
445 in core PC23A (Rella et al., 2012), abundance of benthic foraminifera in the NE
446 Pacific, an indicator of anoxic condition (Cannariato and Kennett, 1999), abundance
447 of *Pulleniatina obliquiloculata*, an indicator of the Kuroshio strength (Shi et al., 2014)
448 (Figure 6).

449 **6.2.1. Effects of regional ocean temperature on deglacial deoxygenation**

450 Warming ocean temperatures lead to lower oxygen solubility. In the geological
451 past, solubility effects connected to temperature changes of the water column thought
452 to enhance or even trigger hypoxia (Praetorius et al., 2015). For instance, Shi et al.
453 (2014) reported an increase in SST of around 4°C (~21°C to ~24.6°C) during the last
454 deglaciation in core CSH1. Based on thermal solubility effects, a hypothetical
455 warming of 1°C at our site would reduce oxygen concentrations by about 8 μM
456 (Benson and Krause, 1984), which could drive a drastic drop of oxygen concentration
457 by <30 μM in subsurface water of the OT. Therefore, we assume that the late
458 deglacial hypoxia in the OT underwent a similar increase in ocean temperatures.



459 However, given the semi-quantitative nature of our data about oxygenation changes,
460 which seemingly exceed an amplitude of $>30 \mu\text{M}$, we suggest that other factors, in
461 particular processes like local changes in export productivity, regional influences such
462 as vertical mixing due to changes of the Kuroshio Current, as well as far-field effects
463 all may have played some decisive roles in shaping the oxygenation history of the OT.

464 **6.2.2. Links between deglacial primary productivity and sedimentary** 465 **deoxygenation**

466 Previous studies have suggested the occurrence of high primary productivity in
467 the entire OT during the last deglacial period (Chang et al., 2009; Jian et al., 1996;
468 Kao et al., 2008; Li et al., 2017; Shao et al., 2016; Wahyudi and Minagawa, 1997).
469 Such an increase in export production was due to favorable conditions for bloom
470 development, which were likely induced by warm temperatures and maxima in
471 nutrient availability, the latter being mainly sourced from increased discharge of the
472 Changjiang River, erosion of material from the ongoing flooding of the shallow
473 continental shelf in the ECS, and upwelling of Kuroshio Intermediate Water (Chang
474 et al., 2009; Li et al., 2017; Shao et al., 2016; Wahyudi and Minagawa, 1997). On the
475 basis of sedimentary reactive phosphorus concentration, Li et al. (2017) concluded
476 that export productivity increased during warm episodes but decreased during cold
477 spells on millennial timescales over the last 91 ka in the OT. Gradually increasing
478 concentrations of CaCO_3 in core CSH1 during the deglaciation (Figure 6a) and little
479 changes in foraminiferal fragmentation ratios (Wu et al., 2004), are indicative of high
480 export productivity in the northern OT. Accordingly, our data indicate that an increase
481 in export productivity, which was previously reported from the middle and southern
482 OT during the last deglaciation, and thus was a pervasive, synchronous phenomenon
483 of entire study region at the outermost extension of the ECS.

484 As a consequence, high export productivity lowers oxygen concentrations in
485 deeper waters, due to subsurface consumption of oxygen by remineralization of
486 organic matter. Similar events of high export productivity have been extensively
487 reported in the entire North Pacific due to increased nutrient supply, high SST,
488 reduced sea ice cover, etc. (Crusius et al., 2004; Dean et al., 1997; Jaccard and



489 Galbraith, 2012; Kohfeld and Chase, 2011). In most of these cases, the increases in
490 productivity were likely also responsible for oxygen depletion in mid-depth waters,
491 due to exceptionally high oxygen consumption. However, the productivity changes
492 during the deglacial interval, very specifically CaCO_3 , are not fully consistent with the
493 trends of excess U and Mo/Mn ratio (Figure 4). The sedimentary oxygenation thus
494 cannot be determined by export productivity alone.

495 **6.2.3 Effects of the Kuroshio dynamics on sedimentary oxygenation**

496 The Kuroshio Current, one of the main drivers of vertical mixing, has been
497 identified as the key factor in controlling modern deep ventilation in the Okinawa
498 Trough (Kao et al., 2006). However, the flow path of the Kuroshio in the Okinawa
499 Trough during the glacial interval remains a matter of debate. Planktic foraminiferal
500 assemblages in sediment cores from inside and outside the Okinawa Trough indicated
501 that the Kuroshio have migrated to the east of the Ryukyu Islands during the LGM
502 (Ujiié and Ujiié, 1999). Subsequently, Kao et al. (2006) based on modeling results
503 suggested that the Kuroshio still enters into the Okinawa Trough, but the volume
504 transport was reduced by 43% compared to the present-day transport and the outlet of
505 Kuroshio switches from the Tokara Strait to the Kerama Gap at -80 and -135m
506 lowered sea level. Combined with sea surface temperature (SST) records and ocean
507 model results, Lee et al. (2013) argued that there was little effect of deglacial sea-level
508 change on the path of the Kuroshio, which still exited the Okinawa Trough from the
509 Tokara Strait during the glacial period. Because the main stream of the Kuroshio
510 Current is at a water depth of ~150 m, the SST records are insufficient to decipher past
511 changes of the Kuroshio (Ujiié et al., 2016). On the other hand, low abundances of *P.*
512 *obliquiloculata* in core CSH1 in the northern OT (Figure 6e) indicate that the main
513 flow path of the Kuroshio may have migrated to the east of the Ryukyu Island (Shi et
514 al., 2014). Such a flow change would have been caused by the proposed block of the
515 Ryukyu-Taiwan land bridge by low sea level (Ujiié and Ujiié, 1999) and an overall
516 reduced Kuroshio intensity (Kao et al., 2006), effectively suppressing the effect of the
517 Kuroshio on deep ventilation in the OT. Our RSEs data show that oxygenated
518 sedimentary conditions were dominant in the northern OT throughout the last glacial



519 period (Figures 6a, b, c, d). The Kuroshio thus likely had a weak or even no effect on
520 the renewal of oxygen to the sedimentary environment during the last glacial period.

521 On the other hand, the gradually increasing abundance of *P.obliquiloculata*
522 (Figure 6e) from 15 ka onwards indicates an intensified Kuroshio Current. Matsumoto
523 et al. (2002) suggested that the influence of the present Kuroshio can reach to the
524 bottom depth of the permanent thermocline, which is approximately at 1000 m water
525 depth. However, as mentioned above, the effect of Kuroshio on the sedimentary
526 oxygenation was likely very limited during glacial period and only gradually
527 increasing throughout the last glacial termination. Therefore, while its effect on our
528 observed deglacial variation in oxygenation may provide a slowly changing
529 background condition in vertical mixing effects on the sedimentary oxygenation in the
530 OT, it cannot account for the first order, rapid oxygenation changes that we observe
531 between 18 and 9 ka, including indications for millennial-scale variations (Figure 6).

532 Better oxygenated sedimentary conditions since 8.5 ka coincided with intensified
533 Kuroshio (Shi et al., 2014; Ujiie et al., 2003), as indicated by rapidly increased SST
534 and *P. obliquiloculata* abundance in core CSH1 (Figure 6e). The re-entrance of the
535 Kuroshio into the OT (Shi et al., 2014) with rising eustatic sea level likely enhanced
536 the vertical mixing and exchange between bottom and surface waters, ventilating the
537 deep water in the OT. Previous comparative studies based on epibenthic $\delta^{13}\text{C}$ values
538 indicated well-ventilated deep water feeding both inside the OT and outside off the
539 Ryukyu Islands during the Holocene (Kubota et al., 2010; Wahyudi and Minagawa,
540 1997). In summary, during the Holocene our observed enhanced sedimentary
541 oxygenation regime is mainly related to the intensified Kuroshio, while the effect of
542 the Kuroshio on OT oxygenation was limited before 15 ka.

543 **6.2.4. Effects of GNPIW on sedimentary oxygenation**

544 Relatively stronger oxygenated Glacial North Pacific Intermediate Water
545 (GNPIW), coined by (Matsumoto et al., 2002), has been widely documented in the
546 Bering Sea (Itaki et al., 2012; Kim et al., 2011; Rella et al., 2012), the Okhotsk Sea
547 (Itaki et al., 2008; Okazaki et al., 2014; Okazaki et al., 2006; Wang and Wang, 2008;
548 Wu et al., 2014), off east Japan (Shibahara et al., 2007), the eastern North Pacific



549 (Cartapanis et al., 2011; Ohkushi et al., 2013) and western subarctic Pacific (Keigwin,
550 1998; Matsumoto et al., 2002). The intensified ventilation of GNPIW is firstly
551 attributable to the displacement of formation source region to the Bering Sea
552 (Ohkushi et al., 2003) and then is further confirmed by Horikawa et al. (2010). Under
553 such conditions, the invasion of well-ventilated GNPIW into the OT through the
554 Kerama Gap would have replenished the water column oxygen in the OT, although
555 the penetration depth of GNPIW remains under debate (Jaccard and Galbraith, 2013;
556 Okazaki et al., 2010; Rae et al., 2014). Both a gradual decrease in excess U
557 concentration and an increase in Mo/Mn ratio during the last glacial period (25-50 ka)
558 validate such inference, suggesting pronounced effects of intensified GNPIW in the
559 OT.

560 During HS1, a stronger formation of GNPIW was recorded in the North Pacific
561 by a variety of studies. On the basis of paired benthic-planktic (B-P) ^{14}C data and
562 model simulations, Okazaki et al. (2010) suggested that NPIW penetrated into a water
563 depth of ~2500 to 3000 m during HS1. In contrast, Max et al. (2014) argued against
564 deep water formation in the North Pacific and showed that GNPIW was
565 well-ventilated only to intermediate water depths (< 1400 m). Various mid- and
566 high-latitude North Pacific records of B-P ^{14}C age offsets at the intermediate water
567 depth (<600–2000 m) showed an active production of GNPIW during HS1 (Max et al.,
568 2014; Sagawa and Ikehara, 2008). Moreover, Kubota et al. (2010) reported increased
569 subsurface water temperatures related to enhanced GNPIW contributions during HS1
570 at a water depth of 1166m (GH08, and young deep water was observed in the northern
571 South China Sea during HS1 (Wan and Jian, 2014).

572 All these multiple lines of evidence imply the presence of well-ventilated
573 intermediate water in the upper 2000 m of the North Pacific during HS1. At this point,
574 the effect of a strong GNPIW likely reached the South China Sea (Wan and Jian, 2014;
575 Zheng et al., 2016), further to the south the Okinawa Trough. The pathway of GNPIW
576 from numerical model simulations (Zheng et al., 2016) was similar to modern
577 observations (You, 2003). Thus, a persistent, cause and effect relation has been
578 established between GNPIW ventilation, the oxygen concentration of OT deepwater



579 and sediment redox state during HS1. In addition, our data also suggested a similarly
580 enhanced ventilation in HS2 (Figure 6) that must also be attributed to intensified
581 GNPIW.

582 Hypoxic conditions during Bölling-Alleröd (B/A) have been also widely
583 observed in the mid- and high-latitude North Pacific (Jaccard and Galbraith, 2012;
584 Praetorius et al., 2015). Our data, both excess U concentrations and Mo/Mn ratio
585 recorded in core CSH1 (Figures 6b-d), further reveal the expansion of
586 oxygen-depletion at mid-depth waters down to the subtropical NW Pacific during the
587 late deglacial period. Based on high relative abundances of radiolarian species,
588 indicators of upper intermediate water ventilation in core PC-23A, Itaki et al. (2012)
589 suggested that a presence of well-ventilated waters was limited to the upper
590 intermediate layer (200–500 m) in the Bering Sea during warm periods, such as the
591 B/A and Preboreal. Higher B-P foraminiferal ^{14}C ages, together with increased
592 intermediate water temperature and salinity recorded in core GH02-1030 (off East
593 Japan) supported a weakened formation of NPIW during the B/A (Sagawa and
594 Ikehara, 2008). These lines of evidence indicate that the boundary between GNPIW
595 and North Pacific Deep Water shoaled during the B/A, in comparison to HS1. Based
596 on a comparison of two benthic foraminiferal oxygen and carbon isotope records from
597 off northern Japan and the southern Ryukyu Island, Kubota et al. (2010) found a
598 stronger influence of Pacific Deep Water on intermediate-water temperature and
599 ventilation at their southern than the northern locations, although both sites are
600 located at similar water depths (1166 m and 1212 m, respectively). Higher excess U
601 concentration and low Mo/Mn ratio in our core CSH1 during the B/A and Preboreal
602 suggest reduced sedimentary oxygenation, consistent with reduced ventilation of
603 GNPIW, contributing to the subsurface water suboxia in the OT.

604 During the YD, Mo/Mn ratio and excess U show a slightly decreased oxygen
605 condition in the northern OT. In contrast, benthic foraminiferal $\delta^{18}\text{O}$ and $\delta^{13}\text{C}$ values
606 in a sediment core collected from the Oyashio region suggested a strengthened
607 formation and ventilation of GNPIW during the YD (Ohkushi et al., 2016). This
608 pattern possibly indicates a time-dependent, varying contribution of distal GNPIW to



609 the deglacial OT oxygenation history, and we presume a more pronounced
610 contribution of organic matter degradation due to high export productivity during this
611 period, as suggested by increasing CaCO₃ content.

612 **6.3. Subtropical North Pacific ventilation links to North Atlantic Climate**

613 Our RSEs data show a substantial millennial variability in intermediate water
614 ventilation in the subtropical North Pacific. Notably, both enhanced ventilation during
615 HS1 and HS2 and oxygen-poor condition during the B/A respectively correspond to
616 the collapse and resumption of Atlantic meridional overturning circulation (AMOC)
617 (Bohm et al., 2015; McManus et al., 2004) (Figure 7 d). This is consistent with the
618 results of various modeling simulations (Chikamoto et al., 2012; Menviel et al., 2014;
619 Okazaki et al., 2010; Saenko et al., 2004), although these models had different
620 scenarios and causes for the observed effects in GNPIW formation, and ventilation
621 ages derived from B-P¹⁴C (Freeman et al., 2015; Max et al., 2014; Okazaki et al.,
622 2012). These lines of evidence reveal a persistent link between the ventilation of
623 North Pacific and the North Atlantic climate. Such links have also been corroborated
624 by using proxy data and modeling experiment between AMOC and East Asian
625 monsoon during the 8.2 ka event (Liu et al., 2013), the Holocene (Wang et al., 2005)
626 and 34–60 ka (Sun et al., 2012). The mechanism linking East Asia with North
627 Atlantic has been attributed to an atmospheric teleconnection, such as the position and
628 strength of Westerly Jet and Mongolia-Siberian High (Porter and Zhisheng, 1995).
629 However, the mechanism behind such oceanic ventilation seesaw pattern between the
630 North Atlantic and North Pacific is still unclear.

631 Increased NPIW formation of HS1 may have been caused by enhanced
632 salinity-driven vertical mixing through higher meridional water mass transport from
633 the subtropical Pacific. Previous studies have proposed that intermediate water
634 formation in the North Pacific hinged on a basin-wide increase in sea surface salinity
635 driven by changes in strength of the summer EAM and the moisture transport from
636 the Atlantic to the Pacific (Emile-Geay et al., 2003). Several modeling studies found
637 that freshwater forcing in the North Atlantic could cause a widespread surface
638 salinification in the subtropical Pacific Ocean (Menviel et al., 2014; Okazaki et al.,



639 2010; Saenko et al., 2004). This idea has been tested by proxy data (Rodríguez-Sanz
640 et al., 2013; Sagawa and Ikehara, 2008), which indicated a weakened summer EAM
641 and reduced transport of moisture from Atlantic to Pacific through Panama Isthmus
642 owing to the southward displacement of ITCZ caused by a weakening of AMOC.
643 Along with this process, as predicted through a general circulation modeling, a
644 strengthened Pacific Meridional Overturning Circulation would have transported
645 more warm and salty subtropical water into the high-latitude North Pacific (Okazaki
646 et al., 2010). In accordance with comprehensive Mg/Ca ratio-based salinity
647 reconstructions, however, Riethdorf et al. (2013) found no clear evidence for such
648 higher salinity patterns in the subarctic northwest Pacific during HS1.

649 On the other hand, a weakened AMOC would deepen the wintertime Aleutian
650 Low (Okumura et al., 2009), which is closely related to the sea ice formation in the
651 marginal seas of the subarctic Pacific (Cavaliere and Parkinson, 1987). Intense brine
652 rejection, accompanied by expanded sea ice formation, would have enhanced the
653 NPIW formation. Recently our modeling-derived evidence suggests enhanced sea ice
654 coverage in the southern Okhotsk Sea and off East Kamchatka Peninsula (Gong et al.,
655 2019). In addition, higher advection of low-salinity water via the Alaskan Stream to
656 the subarctic NW Pacific was probably enhanced during HS1, related to a shift of the
657 Aleutian Low pressure system over the North Pacific, which could also increase sea
658 ice formation, brine rejection and thereafter intermediate water ventilation (Riethdorf
659 et al., 2013).

660 During the late deglaciation, ameliorating global climate conditions, such as
661 warming Northern Hemisphere, and a strengthened Asian summer monsoon, are a
662 result of changes in insolation forcing, greenhouse gases concentrations, and variable
663 strengths of the AMOC (Clark et al., 2012; Liu et al., 2009). During the B/A, a
664 decrease in sea ice extent and duration, as well as reduced advection of Alaska Stream
665 waters were indicated by combined reconstructions of SST and mixed layer
666 temperatures from the subarctic Pacific (Riethdorf et al., 2013). At that time, the
667 rising eustatic sea level (Spratt and Lisiecki, 2016) would have supported the
668 intrusion of Alaska Stream into the Bering Sea by deepening and opening glacial



669 closed straits of the Aleutian Islands chain, while reducing the advection of the Alaska
670 Stream to the subarctic Pacific gyre (Riethdorf et al., 2013). In this scenario, saltier
671 and more stratified surface water conditions would have inhibited brine rejection and
672 subsequent formation and ventilation of NPIW (Lam et al., 2013), leading to a
673 reorganization of the Pacific water mass, closely coupled to the collapse and
674 resumption modes of the AMOC during these two intervals.

675 **6.4 Increased storage of CO₂ at mid-depth water in the North Pacific at the B/A**

676 One of the striking features of RSEs data is higher Mo/Mn ratios and excess U
677 concentrations at the B/A, indicating a substantial oxygen-poor condition in the
678 subtropical North Pacific, coinciding with the termination of atmospheric CO₂
679 concentration rise (Marcott et al., 2014) (Figure 7a). As described above, it can be
680 related to the upwelling of nutrient- and CO₂-rich Pacific Deep Water due to
681 resumption of AMOC and enhanced export production. Although here we are unable
682 to distinguish these two reasons from each other, boron isotope data measured on
683 surface-dwelling foraminifera in core MD01-2416 situated in the western subarctic
684 North Pacific did reveal a decrease in near-surface pH and an increase in pCO₂ at this
685 time (Gray et al., 2018). That is to say, subarctic North Pacific is a source of relatively
686 high atmospheric CO₂ concentration at the B/A. Here we cannot conclude that the
687 same processes could have occurred in the subtropical North Pacific due to the lack of
688 well-known drivers to draw out of the old carbon in the deep sea into the atmosphere.
689 However, an expansion of oxygen-depletion zone in the entire North Pacific suggest
690 an increase in respired carbon storage at intermediate-depth in the subtropical North
691 Pacific, which likely stalls the rise of atmospheric CO₂. Our results support the
692 findings by Galbraith et al. (2007) and are consistent with the hypothesis of deglacial
693 flushing of respired carbon dioxide from an isolated, deep ocean reservoir (Marchitto
694 et al., 2007; Sigman and Boyle, 2000). Given the sizeable volume of the North Pacific,
695 potentially, once the respired carbon could be emitted to the atmosphere in stages,
696 which would play an important role in propelling the Earth out of the last ice age
697 (Jaccard and Galbraith, 2018).

698 **7. Conclusions**



699 Our geochemical results revealed substantial changes in intermediate water redox
700 conditions in the northern Okinawa Trough over the last 50ka on orbital and millennial
701 timescales in the past. The sedimentary oxygenation variability presented here
702 provides key evidence for the impact of ventilation of NPIW on the sedimentary
703 oxygenation in the subtropical North Pacific and highlights the major role of Atlantic
704 Meridional Overturning Circulation in regulating the variations in sedimentary
705 oxygenation in the Okinawa Trough through ventilation of NPIW. Combined with
706 other published records, we also suggest an expansion of oxygen-depleted zone and
707 accumulation of respired carbon at the mid-depth waters of the North Pacific at the
708 B/A, coinciding with the termination of atmospheric CO₂ rise. Once the release of the
709 sequestered carbon into the atmosphere in stages, it would be helpful to maintain high
710 atmospheric CO₂ levels during the deglaciation and to propel the earth out of the
711 glacial climate.

712

713 **Data availability.** All raw data are available to all interested researchers upon request.

714

715 **Author Contributions.** J.J.Z. and X.F.S. conceived the study. A.M.Z. performed
716 geochemical analyses of bulk sediments. J.J.Z., X.F.S. K.S. and X.G. led the write up
717 of the manuscript. All other authors provided comments on the manuscript and
718 contributed to the final version of the manuscript.

719

720 **Competing interests:** The authors declare no competing interests.

721

722 **Acknowledgements**

723 Financial support was provided by the National Program on Global Change and
724 Air-Sea Interaction (GASI-GEOGE-04), by the National Natural Science Foundation
725 of China (Grant Nos.: 41476056, 41876065, 41420104005, 41206059, and U1606401)
726 and by the Basic Scientific Fund for National Public Research Institutes of China
727 (No.2016Q09) and International Cooperative Projects in Polar Study (201613) and
728 Taishan Scholars Program of Shandong. This study is a contribution to the bilateral



729 Sino-German collaboration project (funding through BMBF grant 03F0704A –
730 SIGEPAX). XG, LLJ, GL, RT thank the bilateral Sino-German collaboration
731 NOPAWAC project (BMBF grant No. 03F0785A).LLJ and RT acknowledge financial
732 support through the national Helmholtz REKLIM Initiative. We would like to thank
733 the anonymous reviewers, who helped to improve the quality of this manuscript. The
734 data used in this study are available from the authors upon request
735 (zoujianjun@fio.org.cn).

736

737 **References**

- 738 Algeo, T. J.: Can marine anoxic events draw down the trace element inventory of seawater?, *Geology*,
739 32, 1057-1060, 2004.
- 740 Algeo, T. J. and Lyons, T. W.: Mo-total organic carbon covariation in modern anoxic marine
741 environments: Implications for analysis of paleoredox and paleohydrographic conditions,
742 *Paleoceanography*, 21, PA1016, doi: 10.1029/2004pa001112, 2006.
- 743 Algeo, T. J. and Tribovillard, N.: Environmental analysis of paleoceanographic systems based on
744 molybdenum–uranium covariation, *Chemical Geology*, 268, 211-225, 2009.
- 745 Benson, B. B. and Krause, D.: The concentration and isotopic fractionation of oxygen dissolved in
746 freshwater and seawater in equilibrium with the atmosphere, *Limnology and Oceanography*, 29,
747 620-632, 1984.
- 748 Bohm, E., Lippold, J., Gutjahr, M., Frank, M., Blaser, P., Antz, B., Fohlmeister, J., Frank, N., Andersen,
749 M. B., and Deininger, M.: Strong and deep Atlantic meridional overturning circulation during the last
750 glacial cycle, *Nature*, 517, 73-76, 2015.
- 751 Burdige, D. J.: The biogeochemistry of manganese and iron reduction in marine sediments,
752 *Earth-Science Reviews*, 35, 249-284, 1993.
- 753 Cannariato, K. G. and Kennett, J. P.: Climatically related millennial-scale fluctuations in strength of
754 California margin oxygen-minimum zone during the past 60 k.y, *Geology*, 27, 975-978, 1999.
- 755 Cartapanis, O., Tachikawa, K., and Bard, E.: Northeastern Pacific oxygen minimum zone variability
756 over the past 70 kyr: Impact of biological production and oceanic ventilation, *Paleoceanography*, 26,
757 PA4208, doi: 10.1029/2011PA002126, 2011.
- 758 Cavalieri, D. J. and Parkinson, C. L.: On the relationship between atmospheric circulation and the
759 fluctuations in the sea ice extents of the bering and okhotsk seas, *Journal of Geophysical*
760 *Research-Oceans*, 92, 7141-7162, 1987.
- 761 Chang, A. S., Pedersen, T. F., and Hendy, I. L.: Effects of productivity, glaciation, and ventilation on
762 late Quaternary sedimentary redox and trace element accumulation on the Vancouver Island margin,
763 western Canada, *Paleoceanography*, 29, doi: 10.1002/2013PA002581, 2014.
- 764 Chang, Y.-P., Chen, M.-T., Yokoyama, Y., Matsuzaki, H., Thompson, W. G., Kao, S.-J., and Kawahata,
765 H.: Monsoon hydrography and productivity changes in the East China Sea during the past 100,000
766 years: Okinawa Trough evidence (MD012404), *Paleoceanography*, 24, PA3208, doi:
767 10.1029/2007PA001577, 2009.
- 768 Chen, J., Zhang, D., Zhang, W., and Li, T.: The paleoclimatic change since the last glacialiation in the



- 769 north of Okinawa Trough based on the spore-pollen records, *Acta Oceanologica Sinica*, 28, 85-91,
770 2006 (in Chinese with English Abstract).
- 771 Cheng, H., Edwards, R. L., Sinha, A., Spötl, C., Yi, L., Chen, S., Kelly, M., Kathayat, G., Wang, X., Li,
772 X., Kong, X., Wang, Y., Ning, Y., and Zhang, H.: The Asian monsoon over the past 640,000 years and
773 ice age terminations, *Nature*, 534, 640-646, 2016.
- 774 Cheng, H., Edwards, R. L., Southon, J., Matsumoto, K., Feinberg, J. M., Sinha, A., Zhou, W., Li, H., Li,
775 X., Xu, Y., Chen, S., Tan, M., Wang, Q., Wang, Y., and Ning, Y.: Atmospheric $14C/12C$ changes during
776 the last glacial period from Hulu Cave, *Science*, 362, 1293-1297, 2018.
- 777 Chikamoto, M. O., Menviel, L., Abe-Ouchi, A., Ohgaito, R., Timmermann, A., Okazaki, Y., Harada, N.,
778 Oka, A., and Mouchet, A.: Variability in North Pacific intermediate and deep water ventilation during
779 Heinrich events in two coupled climate models, *Deep Sea Research Part II: Topical Studies in*
780 *Oceanography*, 61-64, 114-126, 2012.
- 781 Clark, P. U., Shakun, J. D., Baker, P. A., Bartlein, P. J., Brewer, S., Brook, E., Carlson, A. E., Cheng, H.,
782 Kaufman, D. S., Liu, Z., Marchitto, T. M., Mix, A. C., Morrill, C., Otto-Bliesner, B. L., Pahnke, K.,
783 Russell, J. M., Whitlock, C., Adkins, J. F., Blois, J. L., Clark, J., Colman, S. M., Curry, W. B., Flower,
784 B. P., He, F., Johnson, T. C., Lynch-Stieglitz, J., Markgraf, V., McManus, J., Mitrovica, J. X., Moreno, P.
785 I., and Williams, J. W.: Global climate evolution during the last deglaciation, *Proceedings of the*
786 *National Academy of Sciences of the United States of America*, 109, E1134-E1142, 2012.
- 787 Clemens, S. C., Holbourn, A., Kubota, Y., Lee, K. E., Liu, Z., Chen, G., Nelson, A., and Fox-Kemper,
788 B.: Precession-band variance missing from East Asian monsoon runoff, *Nature Communications*, 9,
789 3364, doi: 3310.1038/s41467-41018-05814-41460, 2018.
- 790 Crusius, J., Calvert, S., Pedersen, T., and Sage, D.: Rhenium and molybdenum enrichments in
791 sediments as indicators of oxic, suboxic and sulfidic conditions of deposition, *Earth and Planetary*
792 *Science Letters*, 145, 65-78, 1996.
- 793 Crusius, J., Pedersen, T. F., Kienast, S., Keigwin, L., and Labeyrie, L.: Influence of northwest Pacific
794 productivity on North Pacific Intermediate Water oxygen concentrations during the Boiling-Allerod
795 interval (14.7-12.9 ka), *Geology*, 32, 633-636, 2004.
- 796 Dahl, T. W., Anbar, A. D., Gordon, G. W., Rosing, M. T., Frei, R., and Canfield, D. E.: The behavior of
797 molybdenum and its isotopes across the chemocline and in the sediments of sulfidic Lake Cadagno,
798 Switzerland, *Geochimica et Cosmochimica Acta*, 74, 144-163, 2010.
- 799 Dean, W. E., Gardner, J. V., and Piper, D. Z.: Inorganic geochemical indicators of glacial-interglacial
800 changes in productivity and anoxia on the California continental margin, *Geochimica et Cosmochimica*
801 *Acta*, 61, 4507-4518, 1997.
- 802 Delcroix, T. and Murtugudde, R.: Sea surface salinity changes in the East China Sea during 1997–2001:
803 Influence of the Yangtze River, *Journal of Geophysical Research: Oceans*, 107, 8008,
804 doi:8010.1029/2001JC000893, 2002.
- 805 Dou, Y., Yang, S., Li, C., Shi, X., Liu, J., and Bi, L.: Deepwater redox changes in the southern Okinawa
806 Trough since the last glacial maximum, *Progress in Oceanography*, 135, 77-90, 2015.
- 807 Emile-Geay, J., Cane, M. A., Naik, N., Seager, R., Clement, A. C., and van Geen, A.: Warren revisited:
808 Atmospheric freshwater fluxes and “Why is no deep water formed in the North Pacific”, *Journal of*
809 *Geophysical Research: Oceans*, 108, 3178, 2003.
- 810 Freeman, E., Skinner, L. C., Tisserand, A., Dokken, T., Timmermann, A., Menviel, L., and Friedrich, T.:
811 An Atlantic–Pacific ventilation seesaw across the last deglaciation, *Earth and Planetary Science Letters*,
812 424, 237-244, 2015.



- 813 Galbraith, E. D., Jaccard, S. L., Pedersen, T. F., Sigman, D. M., Haug, G. H., Cook, M., Southon, J. R.,
814 and Francois, R.: Carbon dioxide release from the North Pacific abyss during the last deglaciation,
815 *Nature*, 449, 890-893, 2007.
- 816 Galbraith, E. D., Kienast, M., Pedersen, T. F., and Calvert, S. E.: Glacial-interglacial modulation of the
817 marine nitrogen cycle by high-latitude O₂ supply to the global thermocline, *Paleoceanography*, 19,
818 PA4007, doi:4010.1029/2003PA001000, 2004.
- 819 Ge, S., Shi, X., Wu, Y., Lee, T., Xiong, Y., and Saito, Y.: Rock magnetic property of gravity core CSH1
820 from the northern Okinawa Trough and the effect of early diagenesis, *Acta Oceanologica Sinica*, 26,
821 54-65, 2007.
- 822 Gong, X., Lembke-Jene, L., Lohmann, G., Knorr, G., Tiedemann, R., Zou, J. J., and Shi, X. F.:
823 Enhanced North Pacific deep-ocean stratification by stronger intermediate water formation during
824 Heinrich Stadial 1, *Nature Communications*, 10, 656, doi:610.1038/s41467-41019-08606-41462, 2019.
- 825 Gray, W. R., Rae, J. W. B., Wills, R. C. J., Shevenell, A. E., Taylor, B., Burke, A., Foster, G. L., and
826 Lear, C. H.: Deglacial upwelling, productivity and CO₂ outgassing in the North Pacific Ocean, *Nature*
827 *Geoscience*, 11, 340-344, 2018.
- 828 Helz, G. R., Miller, C. V., Charnock, J. M., Mosselmans, J. F. W., Patrick, R. A. D., Garner, C. D., and
829 Vaughan, D. J.: Mechanism of molybdenum removal from the sea and its concentration in black shales:
830 EXAFS evidence, *Geochimica et Cosmochimica Acta*, 60, 3631-3642, 1996.
- 831 Hofmann, A. F., Peltzer, E. T., Walz, P. M., and Brewer, P. G.: Hypoxia by degrees: Establishing
832 definitions for a changing ocean, *Deep Sea Research Part I: Oceanographic Research Papers*, 58,
833 1212-1226, 2011.
- 834 Horikawa, K., Asahara, Y., Yamamoto, K., and Okazaki, Y.: Intermediate water formation in the Bering
835 Sea during glacial periods: Evidence from neodymium isotope ratios, *Geology*, 38, 435-438, 2010.
- 836 Ichikawa, H. and Beardsley, R. C.: The Current System in the Yellow and East China Seas, *Journal of*
837 *Oceanography*, 58, 77-92, 2002.
- 838 Itaki, T., Khim, B. K., and Ikehara, K.: Last glacial-Holocene water structure in the southwestern
839 Okhotsk Sea inferred from radiolarian assemblages, *Marine Micropaleontology*, 67, 191-215, 2008.
- 840 Itaki, T., Kim, S., Rella, S. F., Uchida, M., Tada, R., and Khim, B. K.: Millennial-scale variations of
841 late Pleistocene radiolarian assemblages in the Bering Sea related to environments in shallow and deep
842 waters, *Deep-Sea Research Part II-Topical Studies in Oceanography*, 61-64, 127-144, 2012.
- 843 Ivanochko, T. S. and Pedersen, T. F.: Determining the influences of Late Quaternary ventilation and
844 productivity variations on Santa Barbara Basin sedimentary oxygenation: a multi-proxy approach,
845 *Quaternary Science Reviews*, 23, 467-480, 2004.
- 846 Jaccard, S. L. and Galbraith, E. D.: Direct ventilation of the North Pacific did not reach the deep ocean
847 during the last deglaciation, *Geophysical Research Letters*, 40, 199-203, 2013.
- 848 Jaccard, S. L. and Galbraith, E. D.: Large climate-driven changes of oceanic oxygen concentrations
849 during the last deglaciation, *Nature Geoscience*, 5, 151-156, 2012.
- 850 Jaccard, S. L. and Galbraith, E. D.: Push from the Pacific, *Nature Geoscience*, 11, 299-300, 2018.
- 851 Jaccard, S. L., Galbraith, E. D., Martínez-García, A., and Anderson, R. F.: Covariation of deep
852 Southern Ocean oxygenation and atmospheric CO₂ through the last ice age, *Nature*, 530, 207-210,
853 2016.
- 854 Jaccard, S. L., Galbraith, E. D., Sigman, D. M., Haug, G. H., Francois, R., Pedersen, T. F., Dulski, P.,
855 and Thierstein, H. R.: Subarctic Pacific evidence for a glacial deepening of the oceanic respired carbon
856 pool, *Earth and Planetary Science Letters*, 277, 156-165, 2009.



- 857 Jian, Z. M., Chen, R. H., and Li, B. H.: Deep-sea benthic foraminiferal record of the paleoceanography
858 in the southern Okinawa trough over the last 20000 years, *Science in China Series D-Earth Sciences*,
859 39, 551-560, 1996.
- 860 Kao, S. J., Horng, C. S., Hsu, S. C., Wei, K. Y., Chen, J., and Lin, Y. S.: Enhanced deepwater
861 circulation and shift of sedimentary organic matter oxidation pathway in the Okinawa Trough since the
862 Holocene, *Geophysical Research Letters*, 32, L15609, doi:10.1029/12005GL023139, 2005.
- 863 Kao, S. J., Liu, K. K., Hsu, S. C., Chang, Y. P., and Dai, M. H.: North Pacific-wide spreading of
864 isotopically heavy nitrogen during the last deglaciation: Evidence from the western Pacific,
865 *Biogeosciences*, 5, 1641-1650, 2008.
- 866 Kao, S. J., Wu, C.-R., Hsin, Y.-C., and Dai, M.: Effects of sea level change on the upstream Kuroshio
867 Current through the Okinawa Trough, *Geophysical Research Letters*, 33, L16604,
868 doi:10.1029/12006gl026822, 2006.
- 869 Keigwin, L. D.: Glacial-age hydrography of the far northwest Pacific Ocean, *Paleoceanography*, 13,
870 323-339, 1998.
- 871 Kim, S., Khim, B. K., Uchida, M., Itaki, T., and Tada, R.: Millennial-scale paleoceanographic events
872 and implication for the intermediate-water ventilation in the northern slope area of the Bering Sea
873 during the last 71 kyrs, *Global and Planetary Change*, 79, 89-98, 2011.
- 874 Klinkhammer, G. P. and Palmer, M. R.: Uranium in the oceans: Where it goes and why, *Geochimica et*
875 *Cosmochimica Acta*, 55, 1799-1806, 1991.
- 876 Kohfeld, K. E. and Chase, Z.: Controls on deglacial changes in biogenic fluxes in the North Pacific
877 Ocean, *Quaternary Science Reviews*, 30, 3350-3363, 2011.
- 878 Kubota, Y., Kimoto, K., Tada, R., Oda, H., Yokoyama, Y., and Matsuzaki, H.: Variations of East Asian
879 summer monsoon since the last deglaciation based on Mg/Ca and oxygen isotope of planktic
880 foraminifera in the northern East China Sea, *Paleoceanography*, 25, PA4205,
881 doi:10.1029/2009pa001891, 2010.
- 882 Lam, P. J., Robinson, L. F., Blusztajn, J., Li, C., Cook, M. S., McManus, J. F., and Keigwin, L. D.:
883 Transient stratification as the cause of the North Pacific productivity spike during deglaciation, *Nature*
884 *Geosci*, 6, 622-626, 2013.
- 885 Lee, K. E., Lee, H. J., Park, J.-H., Chang, Y.-P., Ikehara, K., Itaki, T., and Kwon, H. K.: Stability of the
886 Kuroshio path with respect to glacial sea level lowering, *Geophysical Research Letters*, 40, 392-396,
887 doi:10.1002/grl.50102, 2013.
- 888 Li, D., Zheng, L.-W., Jaccard, S. L., Fang, T.-H., Paytan, A., Zheng, X., Chang, Y.-P., and Kao, S.-J.:
889 Millennial-scale ocean dynamics controlled export productivity in the subtropical North Pacific,
890 *Geology*, 45, 651-654, 2017.
- 891 Li, T. G., Xiang, R., Sun, R. T., and Cao, Q. Y.: Benthic foraminifera and bottom water evolution in the
892 middle-southern Okinawa Trough during the last 18 ka, *Science in China Series D-Earth Sciences*, 48,
893 805-814, 2005.
- 894 Li, Y. H. and Schoonmaker, J. E.: Chemical Composition and Mineralogy of Marine Sediments. In:
895 *Treatise on Geochemistry (Second Edition)*, Turekian, K. K. (Ed.), Elsevier, Oxford, 2014.
- 896 Liu, Y. H., Henderson, G. M., Hu, C. Y., Mason, A. J., Charnley, N., Johnson, K. R., and Xie, S. C.:
897 Links between the East Asian monsoon and North Atlantic climate during the 8,200 year event, *Nature*
898 *Geosci*, 6, 117-120, 2013.
- 899 Liu, Z., Otto-Bliesner, B. L., He, F., Brady, E. C., Tomas, R., Clark, P. U., Carlson, A. E.,
900 Lynch-Stieglitz, J., Curry, W., Brook, E., Erickson, D., Jacob, R., Kutzbach, J., and Cheng, J.: Transient



- 901 Simulation of Last Deglaciation with a New Mechanism for Bølling-Allerød Warming, *Science*, 325,
902 310-314, 2009.
- 903 Lu, Z., Hoogakker, B. A. A., Hillenbrand, C.-D., Zhou, X., Thomas, E., Gutchess, K. M., Lu, W., Jones,
904 L., and Rickaby, R. E. M.: Oxygen depletion recorded in upper waters of the glacial Southern Ocean,
905 *Nature Communication*, 7, doi: 10.1038/ncomms11146, 2016.
- 906 Lyons, T. W., Anbar, A. D., Severmann, S., Scott, C., and Gill, B. C.: Tracking Euxinia in the Ancient
907 Ocean: A Multiproxy Perspective and Proterozoic Case Study, *Annual Review of Earth and Planetary*
908 *Sciences*, 37, 507-534, 2009.
- 909 Machida, H.: The stratigraphy, chronology and distribution of distal marker-tephras in and around
910 Japan, *Global and Planetary Change*, 21, 71-94, 1999.
- 911 Maithani, P. B. and Srinivasan, S.: Felsic Volcanic Rocks, a Potential Source of Uranium - An Indian
912 Overview, *Energy Procedia*, 7, 163-168, 2011.
- 913 Marchitto, T. M., Lehman, S. J., Ortiz, J. D., Flückiger, J., and van Geen, A.: Marine Radiocarbon
914 Evidence for the Mechanism of Deglacial Atmospheric CO₂ Rise, *Science*, 316, 1456-1459, 2007.
- 915 Marcott, S. A., Bauska, T. K., Buizert, C., Steig, E. J., Rosen, J. L., Cuffey, K. M., Fudge, T. J.,
916 Severinghaus, J. P., Ahn, J., Kalk, M. L., McConnell, J. R., Sowers, T., Taylor, K. C., White, J. W. C.,
917 and Brook, E. J.: Centennial-scale changes in the global carbon cycle during the last deglaciation,
918 *Nature*, 514, 616-619, 2014.
- 919 Matsumoto, K., Oba, T., Lynch-Stieglitz, J., and Yamamoto, H.: Interior hydrography and circulation of
920 the glacial Pacific Ocean, *Quaternary Science Reviews*, 21, 1693-1704, 2002.
- 921 Max, L., Lembke-Jene, L., Riethdorf, J. R., Tiedemann, R., Nurnberg, D., Kuhn, H., and Mackensen,
922 A.: Pulses of enhanced North Pacific Intermediate Water ventilation from the Okhotsk Sea and Bering
923 Sea during the last deglaciation, *Climate of the Past*, 10, 591-605, 2014.
- 924 McManus, J., Berelson, W. M., Klinkhammer, G. P., Hammond, D. E., and Holm, C.: Authigenic
925 uranium: Relationship to oxygen penetration depth and organic carbon rain, *Geochimica et*
926 *Cosmochimica Acta*, 69, 95-108, 2005.
- 927 McManus, J. F., Francois, R., Gherardi, J. M., Keigwin, L. D., and Brown-Leger, S.: Collapse and rapid
928 resumption of Atlantic meridional circulation linked to deglacial climate changes, *Nature*, 428, 834-837,
929 2004.
- 930 Menviel, L., England, M. H., Meissner, K. J., Mouchet, A., and Yu, J.: Atlantic-Pacific seesaw and its
931 role in outgassing CO₂ during Heinrich events, *Paleoceanography*, 29, 58-70, 2014.
- 932 Morford, J. L. and Emerson, S.: The geochemistry of redox sensitive trace metals in sediments,
933 *Geochimica et Cosmochimica Acta*, 63, 1735-1750, 1999.
- 934 Nakamura, H., Nishina, A., Liu, Z. J., Tanaka, F., Wimbush, M., and Park, J. H.: Intermediate and deep
935 water formation in the Okinawa Trough, *Journal of Geophysical Research-Oceans*, 118, 6881-6893,
936 2013.
- 937 Nameroff, T. J., Balistrieri, L. S., and Murray, J. W.: Suboxic trace metal geochemistry in the Eastern
938 Tropical North Pacific, *Geochimica et Cosmochimica Acta*, 66, 1139-1158, 2002.
- 939 Nameroff, T. J., Calvert, S. E., and Murray, J. W.: Glacial-interglacial variability in the eastern tropical
940 North Pacific oxygen minimum zone recorded by redox-sensitive trace metals, *Paleoceanography*, 19,
941 PA1010, doi:10.1029/2003PA000912, 2004.
- 942 Nishina, A., Nakamura, H., Park, J.-H., Hasegawa, D., Tanaka, Y., Seo, S., and Hibiya, T.: Deep
943 ventilation in the Okinawa Trough induced by Kerama Gap overflow, *Journal of Geophysical Research:*
944 *Oceans*, 121, 6092-6102, 2016.



- 945 Ohkushi, K., Hara, N., Ikehara, M., Uchida, M., and Ahagon, N.: Intensification of North Pacific
946 intermediate water ventilation during the Younger Dryas, *Geo-Mar Lett*, 36, 353-360, 2016.
- 947 Ohkushi, K., Itaki, T., and Nemoto, N.: Last Glacial-Holocene change in intermediate-water ventilation
948 in the Northwestern Pacific, *Quaternary Science Reviews*, 22, 1477-1484, 2003.
- 949 Ohkushi, K., Kennett, J. P., Zeleski, C. M., Moffitt, S. E., Hill, T. M., Robert, C., Beaufort, L., and Behl,
950 R. J.: Quantified intermediate water oxygenation history of the NE Pacific: A new benthic foraminiferal
951 record from Santa Barbara basin, *Paleoceanography*, 28, 453-467, 2013.
- 952 Okazaki, Y., Kimoto, K., Asahi, H., Sato, M., Nakamura, Y., and Harada, N.: Glacial to deglacial
953 ventilation and productivity changes in the southern Okhotsk Sea, *Palaeogeography Palaeoclimatology*
954 *Palaeoecology*, 395, 53-66, 2014.
- 955 Okazaki, Y., Sagawa, T., Asahi, H., Horikawa, K., and Onodera, J.: Ventilation changes in the western
956 North Pacific since the last glacial period, *Climate of the Past*, 8, 17-24, 2012.
- 957 Okazaki, Y., Seki, O., Nakatsuka, T., Sakamoto, T., Ikehara, M., and Takahashi, K.: *Cycladophora*
958 *davisiana* (Radiolaria) in the Okhotsk Sea: A key for reconstructing glacial ocean conditions, *Journal of*
959 *Oceanography*, 62, 639-648, 2006.
- 960 Okazaki, Y., Timmermann, A., Menviel, L., Harada, N., Abe-Ouchi, A., Chikamoto, M. O., Mouchet,
961 A., and Asahi, H.: Deepwater Formation in the North Pacific During the Last Glacial Termination,
962 *Science*, 329, 200-204, 2010.
- 963 Okumura, Y. M., Deser, C., Hu, A., Timmermann, A., and Xie, S.-P.: North Pacific Climate Response to
964 Freshwater Forcing in the Subarctic North Atlantic: Oceanic and Atmospheric Pathways, *Journal of*
965 *Climate*, 22, 1424-1445, 2009.
- 966 Porter, S. C. and Zhisheng, A.: Correlation between climate events in the North Atlantic and China
967 during the last glaciation, *Nature*, 375, 305-308, 1995.
- 968 Praetorius, S. K., Mix, A. C., Walczak, M. H., Wolhowe, M. D., Addison, J. A., and Prah, F. G.: North
969 Pacific deglacial hypoxic events linked to abrupt ocean warming, *Nature*, 527, 362-366, 2015.
- 970 Qu, T. and Lukas, R.: The Bifurcation of the North Equatorial Current in the Pacific, *Journal of*
971 *Physical Oceanography*, 33, 5-18, 2003.
- 972 Rühlemann, C., Müller, P. J., and Schneider, R. R.: Organic Carbon and Carbonate as Paleoproductivity
973 Proxies: Examples from High and Low Productivity Areas of the Tropical Atlantic. In: *Use of Proxies*
974 *in Paleoceanography: Examples from the South Atlantic*, Fischer, G. and Wefer, G. (Eds.), Springer
975 Berlin Heidelberg, Berlin, Heidelberg, 1999.
- 976 Rae, J. W. B., Sarnthein, M., Foster, G. L., Ridgwell, A., Grootes, P. M., and Elliott, T.: Deep water
977 formation in the North Pacific and deglacial CO₂ rise, *Paleoceanography*, 29, 645-667, 2014.
- 978 Reimer, P. J., Bard, E., Bayliss, A., Beck, J. W., Blackwell, P. G., Bronk Ramsey, C., Buck, C. E.,
979 Cheng, H., Edwards, R. L., Friedrich, M., Grootes, P. M., Guilderson, T. P., Hafliadason, H., Hajdas, I.,
980 Hatté, C., Heaton, T. J., Hoffmann, D. L., Hogg, A. G., Hughen, K. A., Kaiser, K. F., Kromer, B.,
981 Manning, S. W., Niu, M., Reimer, R. W., Richards, D. A., Scott, E. M., Southon, J. R., Staff, R. A.,
982 Turney, C. S. M., and van der Plicht, J.: IntCal13 and Marine13 Radiocarbon Age Calibration Curves
983 0–50,000 Years cal BP, *Radiocarbon*, 55, 1869-1887, 2013.
- 984 Rella, S. F., Tada, R., Nagashima, K., Ikehara, M., Itaki, T., Ohkushi, K., Sakamoto, T., Harada, N., and
985 Uchida, M.: Abrupt changes of intermediate water properties on the northeastern slope of the Bering
986 Sea during the last glacial and deglacial period, *Paleoceanography*, 27, PA3203,
987 doi:3210.1029/2011pa002205, 2012.
- 988 Riethdorf, J.-R., Max, L., Nuernberg, D., Lembke-Jene, L., and Tiedemann, R.: Deglacial development



- 989 of (sub) sea surface temperature and salinity in the subarctic northwest Pacific: Implications for
990 upper-ocean stratification, *Paleoceanography*, 28, doi:10.1002/palo.20014, 2013.
- 991 Riethdorf, J.-R., Thibodeau, B., Ikehara, M., Nürnberg, D., Max, L., Tiedemann, R., and Yokoyama, Y.:
992 Surface nitrate utilization in the Bering sea since 180ka BP: Insight from sedimentary nitrogen
993 isotopes, *Deep Sea Research Part II: Topical Studies in Oceanography*, 125-126, 163-176, 2016.
- 994 Rodríguez-Sanz, L., Mortyn, P. G., Herguera, J. C., and Zahn, R.: Hydrographic changes in the tropical
995 and extratropical Pacific during the last deglaciation, *Paleoceanography*, 28, 529-538, 2013.
- 996 Saenko, O. A., Schmittner, A., and Weaver, A. J.: The Atlantic-Pacific seesaw, *Journal of Climate*, 17,
997 2033-2038, 2004.
- 998 Sagawa, T. and Ikehara, K.: Intermediate water ventilation change in the subarctic northwest Pacific
999 during the last deglaciation, *Geophysical Research Letters*, 35, 5, doi: 10.1029/2008gl035133, 2008.
- 1000 Savrda, C. E. and Bottjer, D. J.: Oxygen-related biofacies in marine strata: an overview and update,
1001 *Geological Society, London, Special Publications*, 58, 201-219, 1991.
- 1002 Scott, C. and Lyons, T. W.: Contrasting molybdenum cycling and isotopic properties in euxinic versus
1003 non-euxinic sediments and sedimentary rocks: Refining the paleoproxies, *Chemical Geology*, 324–325,
1004 19-27, 2012.
- 1005 Scott, C., Lyons, T. W., Bekker, A., Shen, Y., Poulton, S. W., Chu, X., and Anbar, A. D.: Tracing the
1006 stepwise oxygenation of the Proterozoic ocean, *Nature*, 452, 456-459, 2008.
- 1007 Shao, H., Yang, S., Cai, F., Li, C., Liang, J., Li, Q., Hyun, S., Kao, S.-J., Dou, Y., Hu, B., Dong, G., and
1008 Wang, F.: Sources and burial of organic carbon in the middle Okinawa Trough during late Quaternary
1009 paleoenvironmental change, *Deep Sea Research Part I: Oceanographic Research Papers*, 118, 46-56,
1010 2016.
- 1011 Shcherbina, A. Y., Talley, L. D., and Rudnick, D. L.: Direct observations of North Pacific ventilation:
1012 Brine rejection in the Okhotsk Sea, *Science*, 302, 1952-1955, 2003.
- 1013 Shi, X., Wu, Y., Zou, J., Liu, Y., Ge, S., Zhao, M., Liu, J., Zhu, A., Meng, X., Yao, Z., and Han, Y.:
1014 Multiproxy reconstruction for Kuroshio responses to northern hemispheric oceanic climate and the
1015 Asian Monsoon since Marine Isotope Stage 5.1 (~88 ka), *Climate of the Past*, 10, 1735-1750, 2014.
- 1016 Shibahara, A., Ohkushi, K., Kennett, J. P., and Ikehara, K.: Late Quaternary changes in intermediate
1017 water oxygenation and oxygen minimum zone, northern Japan: A benthic foraminiferal perspective,
1018 *Paleoceanography*, 22, PA3213, doi:3210.1029/2005pa001234, 2007.
- 1019 Shimmield, G. B. and Price, N. B.: The behaviour of molybdenum and manganese during early
1020 sediment diagenesis — offshore Baja California, Mexico, *Marine Chemistry*, 19, 261-280, 1986.
- 1021 Sibuet, J. C., Letouzey, J., Barbier, F., Charvet, J., Foucher, J. P., Hilde, T. W. C., Kimura, M., Chiao,
1022 L.-Y., Marsset, B., Muller, C., and Stéphan, J. F.: Back Arc Extension in the Okinawa Trough, *Journal*
1023 *of Geophysical Research: Solid Earth*, 92, 14041-14063, 1987.
- 1024 Sigman, D. M. and Boyle, E. A.: Glacial/interglacial variations in atmospheric carbon dioxide, *Nature*,
1025 407, 859-869, 2000.
- 1026 Spratt, R. M. and Lisiecki, L. E.: A Late Pleistocene sea level stack, *Clim. Past*, 12, 1079-1092, 2016.
- 1027 Sun, Y., Clemens, S. C., Morrill, C., Lin, X., Wang, X., and An, Z.: Influence of Atlantic meridional
1028 overturning circulation on the East Asian winter monsoon, *Nature Geosci*, 5, 46-49, 2012.
- 1029 Sun, Y. B., Oppo, D. W., Xiang, R., Liu, W. G., and Gao, S.: Last deglaciation in the Okinawa Trough:
1030 Subtropical northwest Pacific link to Northern Hemisphere and tropical climate, *Paleoceanography*, 20,
1031 PA4005, doi:4010.1029/2004pa001061, 2005.
- 1032 Sundby, B., Martinez, P., and Gobeil, C.: Comparative geochemistry of cadmium, rhenium, uranium,



- 1033 and molybdenum in continental margin sediments, *Geochimica et Cosmochimica Acta*, 68, 2485-2493,
1034 2004.
- 1035 Talley, L. D.: Distribution formation of North Pacific Intermediate water, *Journal of Physical*
1036 *Oceanography*, 23, 517-537, 1993.
- 1037 Talley, L. D.: Hydrographic Atlas of the World Ocean Circulation Experiment (WOCE). In: Volume 2:
1038 Pacific Ocean, Sparrow, M., Chapman, P., and Gould, J. (Eds.), International WOCE Project Office,
1039 Southampton, UK, 2007.
- 1040 Tribouillard, N., Algeo, T. J., Lyons, T., and Riboulleau, A.: Trace metals as paleoredox and
1041 paleoproductivity proxies: An update, *Chemical Geology*, 232, 12-32, 2006.
- 1042 Ujiié, H. and Ujiié, Y.: Late Quaternary course changes of the Kuroshio Current in the Ryukyu Arc
1043 region, northwestern Pacific Ocean, *Marine Micropaleontology*, 37, 23-40, 1999.
- 1044 Ujiié, Y., Asahi, H., Sagawa, T., and Bassinot, F.: Evolution of the North Pacific Subtropical Gyre
1045 during the past 190 kyr through the interaction of the Kuroshio Current with the surface and
1046 intermediate waters, *Paleoceanography*, 31, 1498-1513, 2016.
- 1047 Ujiié, Y., Ujiié, H., Taira, A., Nakamura, T., and Oguri, K.: Spatial and temporal variability of surface
1048 water in the Kuroshio source region, Pacific Ocean, over the past 21,000 years: evidence from
1049 planktonic foraminifera, *Marine Micropaleontology*, 49, 335-364, 2003.
- 1050 Vorlicek, T. P. and Helz, G. R.: Catalysis by mineral surfaces: Implications for Mo geochemistry in
1051 anoxic environments, *Geochimica et Cosmochimica Acta*, 66, 3679-3692, 2002.
- 1052 Wahyudi and Minagawa, M.: Response of benthic foraminifera to organic carbon accumulation rates in
1053 the Okinawa Trough, *Journal of Oceanography*, 53, 411-420, 1997.
- 1054 Wan, S. and Jian, Z.: Deep water exchanges between the South China Sea and the Pacific since the last
1055 glacial period, *Paleoceanography*, 29, 1162-1178, 2014.
- 1056 Wang, W. L. and Wang, L. C.: Reconstruction of oceanographic changes based on the diatom records
1057 of the central Okhotsk Sea over the last 500000 years, *Terrestrial Atmospheric and Oceanic Sciences*,
1058 19, 403-411, 2008.
- 1059 Wang, Y., Cheng, H., Edwards, R. L., He, Y., Kong, X., An, Z., Wu, J., Kelly, M. J., Dykoski, C. A.,
1060 and Li, X.: The Holocene Asian Monsoon: Links to Solar Changes and North Atlantic Climate, *Science*,
1061 308, 854-857, 2005.
- 1062 Wu, Y., Cheng, Z., and Shi, X.: Stratigraphic and carbonate sediment characteristics of Core CSH1
1063 from the northern Okinawa Trough, *Advances in Marine Science*, 22, 163-169, 2004 (in Chinese with
1064 English Abstract).
- 1065 Wu, Y., Shi, X., Zou, J., Cheng, Z., Wang, K., Ge, S., and Shi, F.: Benthic foraminiferal $\delta^{13}\text{C}$
1066 minimum events in the southeastern Okhotsk Sea over the last 180ka, *Chinese Science Bulletin*, 59,
1067 3066-3074, 2014.
- 1068 You, Y. Z.: The pathway and circulation of North Pacific Intermediate Water, *Geophysical Research*
1069 *Letters*, 30, doi:10.1029/2003gl018561, 2003.
- 1070 You, Y. Z., Suginothara, N., Fukasawa, M., Yasuda, I., Kaneko, I., Yoritaka, H., and Kawamiya, M.:
1071 Roles of the Okhotsk Sea and Gulf of Alaska in forming the North Pacific Intermediate Water, *Journal*
1072 *of Geophysical Research-Oceans*, 105, 3253-3280, 2000.
- 1073 You, Y. Z., Suginothara, N., Fukasawa, M., Yoritaka, H., Mizuno, K., Kashino, Y., and Hartoyo, D.:
1074 Transport of North Pacific Intermediate Water across Japanese WOCE sections, *Journal of Geophysical*
1075 *Research-Oceans*, 108, doi: 10.1029/2002jc001662, 2003.
- 1076 Yu, H., Liu, Z. X., Berne, S., Jia, G. D., Xiong, Y. Q., Dickens, G. R., Wei, G. J., Shi, X. F., Liu, J. P.,



1077 and Chen, F. J.: Variations in temperature and salinity of the surface water above the middle Okinawa
1078 Trough during the past 37 kyr, *Palaeogeography Palaeoclimatology Palaeoecology*, 281, 154-164,
1079 2009.

1080 Zheng, X., Kao, S., Chen, Z., Menviel, L., Chen, H., Du, Y., Wan, S., Yan, H., Liu, Z., Zheng, L., Wang,
1081 S., Li, D., and Zhang, X.: Deepwater circulation variation in the South China Sea since the Last Glacial
1082 Maximum, *Geophysical Research Letters*, 43, 8590-8599, 2016.

1083 Zheng, Y., Anderson, R., van Geen, A., and Fleisher, M.: Remobilization of authigenic uranium in
1084 marine sediments by bioturbation, *Geochimica et Cosmochimica Acta*, 66, 1759-1772, 2002.

1085 Zheng, Y., Anderson, R., van Geen, A., and Kuwabara, J.: Authigenic molybdenum formation in marine
1086 sediments: a link to pore water sulfide in the Santa Barbara Basin, *Geochimica et Cosmochimica Acta*,
1087 64, 4165-4178, 2000.

1088 Zou, J., Shi, X., Liu, Y., Liu, J., Selvaraj, K., and Kao, S.-J.: Reconstruction of environmental changes
1089 using a multi-proxy approach in the Ulleung Basin (Sea of Japan) over the last 48 ka, *Journal of*
1090 *Quaternary Science*, 27, 891-900, 2012.

1091



1092 **Captions**

1093 **Table 1.** Locations of different records and their source references discussed in the
1094 text.

1095

1096 **Table 2.** Age control points adopted between planktic $\delta^{18}\text{O}$ of Core CSH1 and
1097 Chinese stalagmite $\delta^{18}\text{O}$ (Cheng et al., 2016) for tuning the age model between 10 ka
1098 and 60 ka in this study. A linear interpolation was assumed between age control
1099 points.

1100

1101 **Figure 1.** (a) Spatial distribution of dissolved oxygen content at 700 m water depth in
1102 the North Pacific. Black arrows denote simplified Kuroshio and Oyashio circulations
1103 and North Pacific Intermediate Water (NPIW) in the North Pacific. The red thick
1104 dashed line indicates transformation of Okhotsk Sea Intermediate Water (OSIW) by
1105 cabbeling the subtropical NPIW along the subarctic-tropical frontal zone (You, 2003).
1106 The light brown solid line with arrow indicates the spreading path of subtropical
1107 NPIW from northeast North Pacific southward toward the low-latitude northwest
1108 North Pacific (You, 2003). Yellow solid lines with arrow represent two passages
1109 through which NPIW enter into the Okinawa Trough. This figure was created with
1110 Ocean Data View (odv.awi.de). (b) Location of sediment core CSH1 investigated in
1111 this study (red diamond). Also shown are locations of sediment cores investigated
1112 previously from the Okinawa Trough (PN-3, E017, 255 and MD012404; white cross
1113 line), the northern and southern Japan (GH08-2004 and GH02-1030), the Bering Sea
1114 (PC-23A) and the northeastern Pacific (ODP167-1017). The detailed information for
1115 these cores can be seen in Table 1.

1116

1117 **Figure 2.** Spatial distribution of sea surface salinity in the East China Sea. (a) summer
1118 (July to September); (b) winter (January to March). Lower sea surface salinity in
1119 summer relative to that of winter indicates strong effects of summer East Asian
1120 Monsoon.

1121



1122 **Figure 3.** (a) Lithology and oxygen isotope ($\delta^{18}\text{O}$) profile of planktic foraminiferal
1123 species *Globigerinoides ruber* (*G.ruber*) in core CSH1. (b) Plot of ages versus depth
1124 for core CSH1. Three known ash layers are indicated by solid red rectangles. (c) Time
1125 series of linear sedimentation rate (LSR) from core CSH1. (d) Comparison of age
1126 model of core CSH1 with Chinese Stalagmite composite $\delta^{18}\text{O}$ curve of (Cheng et al.,
1127 2016). Tie points for CSH1 core chronology (Table 2) in Figures 2b and 2c are
1128 designated by blue and red solid dots.

1129

1130 **Figure 4.** Age versus (a) linear sedimentation rate (LSR), (b) C/N molar ratio, (c)
1131 Total organic carbon (TOC) concentration, (d) Total nitrogen (TN) concentration, (e)
1132 CaCO_3 concentration, (f) Al concentration, (g) Mn concentration, (h) Mo/Mn ratio, (i)
1133 Mo concentration, (j) excess Mo concentration, (k) U concentration and (l) excess U
1134 concentration in core CSH1. Gray and black vertical bars indicate different sediment
1135 intervals in core CSH1. MIS indicates Marine Isotope Stage. 8.2 ka, PB, YD, B/A,
1136 HS1, LGM and HS2 refer to 8,200 year cold event, Preboreal, Younger Dryas, Bölling
1137 - Alleröd, Heinrich Stadial 1, Last Glacial Maximum and Heinrich Stadial 2,
1138 respectively, which were identified in core CSH1. Blue solid diamonds in Figure 3l
1139 indicate the age control points.

1140

1141 **Figure 5.** Scatter plots of $\text{Mo}_{\text{excess}}$ vs Mn concentrations and U_{excess} concentration vs
1142 Mo/Mn ratio at different time intervals in core CSH1. A various correlation is present
1143 in core CSH1 at different time intervals, which shows their complicated geochemical
1144 behaviors. Strong positive correlation between U_{excess} concentration and Mo/Mn ratio
1145 suggest that they are suitable to track redox conditions in the past.

1146

1147 **Figure 6.** Proxy-related reconstructions of intermediate water oxygenation at site
1148 CSH1 (this study) compared with oxygenation records from other locations of the
1149 North Pacific and published climatic and environmental records from the Okinawa
1150 Trough. From top to bottom: (a) CaCO_3 concentration, (b) U_{excess} concentration, (c)
1151 Mo/Mn ratio, (d) Mn concentration and (e) abundance of *P.obliquiloculata* in core



1152 CSH1 (Shi et al., 2014) and (f) $\delta^{15}\text{N}$ of TOC in core MD01-2404 (Kao et al., 2008), (g)
1153 $\delta^{13}\text{C}$ of *C.wuellerstorfi* in core PN-3(Wahyudi and Minagawa, 1997), (h) Dysoxic taxa
1154 (%) in core ODP 167-1017 in the northeastern Pacific (Cannariato and Kennett, 1999)
1155 and (i) $\delta^{13}\text{C}$ of *Uvigerina akitaensis* in core PC23A in the Bering Sea (Rella et al.,
1156 2012). Gray and black vertical bars are the same as those in Figure 4.

1157

1158 **Figure 7.** Proxy records favoring the existence of oceanic ventilation seesaw between
1159 the subtropical North Pacific and North Atlantic during the last deglaciation and
1160 enhanced carbon storage at mid-depth waters. (a) Atmospheric CO_2 concentration
1161 (Marcott et al., 2014) (b) Indicator of strength of Atlantic Meridional Ocean
1162 Circulation ($^{231}\text{Pa}/^{230}\text{Th}$) (Bohm et al., 2015; McManus et al., 2004); (c) benthic $\delta^{13}\text{C}$
1163 record in core PC-23A in the Bering Sea (Rella et al., 2012); (d) Mo/Mn ratio in core
1164 CSH1; (e) U_{excess} concentration in core CH1. Blue diamonds are the same as those in
1165 Figure 3.

1166



Table 1

Label in Figure 1b	Station	Latitude(°N)	Longitude(°E)	Water depth (m)	Area	Reference
	CSH1	31.23	128.72	703	Okinawa Trough	this study
A	PN-3	28.10	127.34	1058	Okinawa Trough	Wahyudi and Minagawa, (1997)
B	MD012404	26.65	125.81	1397	Okinawa Trough	Kao et al., (2008)
C	E017	26.57	126.02	1826	Okinawa Trough	Li et al., (2005)
D	255	25.20	123.12	1575	Okinawa Trough	Jian et al., (1996)
E	GH08-2004	26.21	127.09	1166	East of Ryukyu Island	Kubota et al. (2010)
	GH02-1030	42.23	144.21	1212	Off Japan	Sagawa and Ikehara, (2008)
	PC-23A	60.16	179.46	1002	Bering Sea	Rella et al.,(2012)
	ODP167-1017	34.54	239.11	955	NE Pacific	Cannariato and Kennett, (1999)



1 Table 2

2

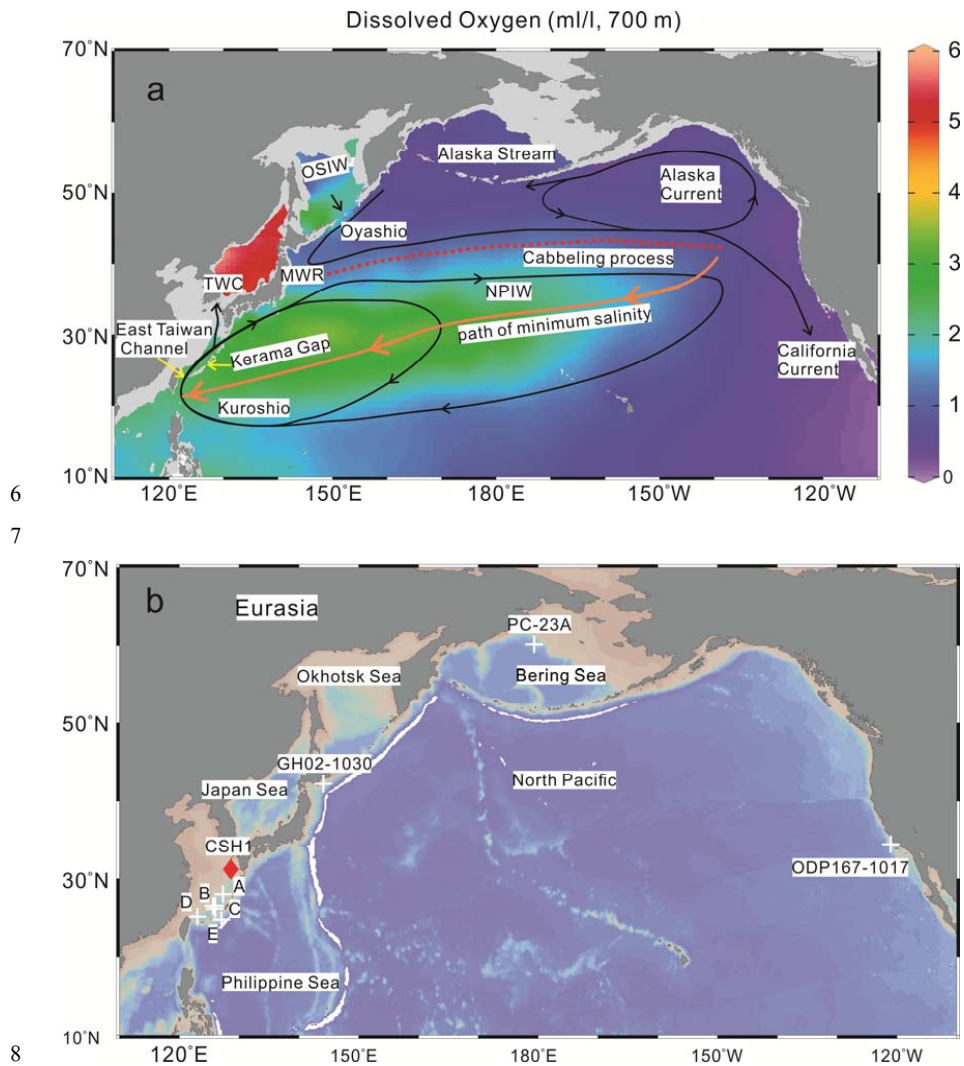
Depth(cm)	AMS ¹⁴ C (yr)	Error (yr)	Calibrated Age (yr)	Tie Point Type	LSR (cm/ka)	Source
10	3420	±35	3296	¹⁴ C		Shi et al., (2014)
106	7060	± 40	7545	¹⁴ C	22.59	Shi et al., (2014)
218			12352	Stalagmite, YD	23.30	This study
322			16029	Stalagmite, H1	28.28	This study
362			19838	Stalagmite	10.50	This study
466			23476	Stalagmite, DO2	28.59	This study
506			24163	Stalagmite, H2	58.22	This study
698			28963	Stalagmite, DO4	40.00	This study
746			29995	Stalagmite, H3	46.51	This study
834			32442	Stalagmite, DO5	35.96	This study
938			37526	Stalagmite, DO8	20.46	This study
978			39468	Stalagmite, H4	20.60	This study
1058			46151	Stalagmite, DO12	11.97	This study
1122			49432	Stalagmite, DO13	19.51	This study
1242			52831	Stalagmite, DO14	35.30	This study
1282			57241	Stalagmite, DO16	9.07	This study
1346			61007	Stalagmite, H6	16.99	This study
1530		±2590	73910	MIS4/5	14.26	Shi et al., (2014)
1610		±3580	79250	MIS 5.1	14.98	Shi et al., (2014)

3

4

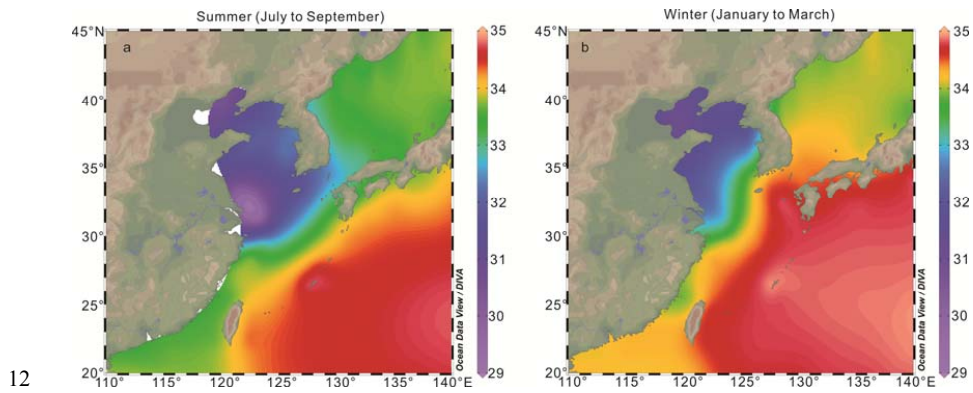


5 Fig.1





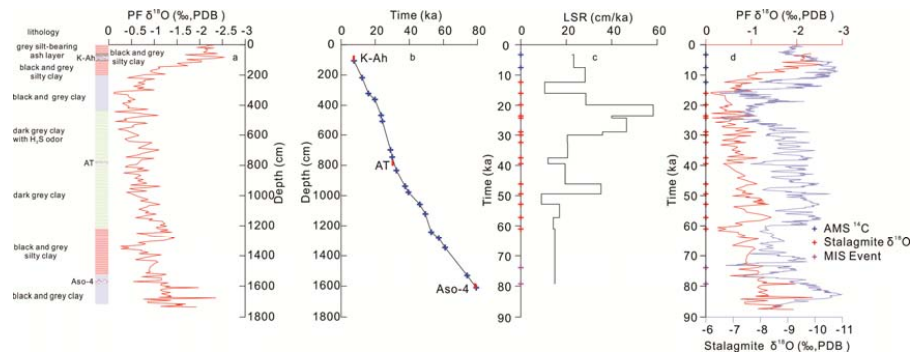
11 Fig.2



12

13

14 Fig.3

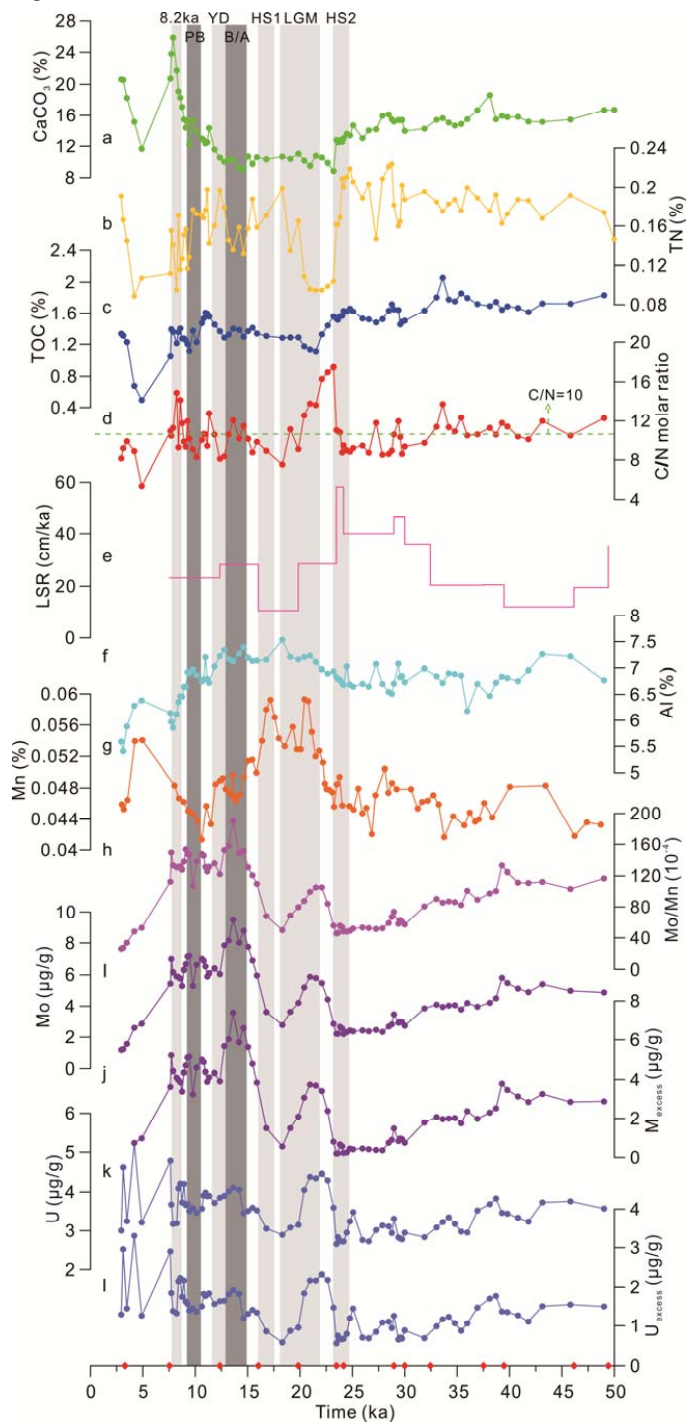


15

16



17 Fig.4



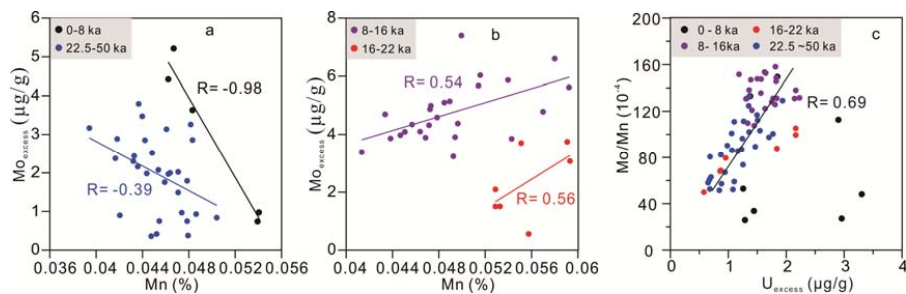
18

19



20

21 Fig.5

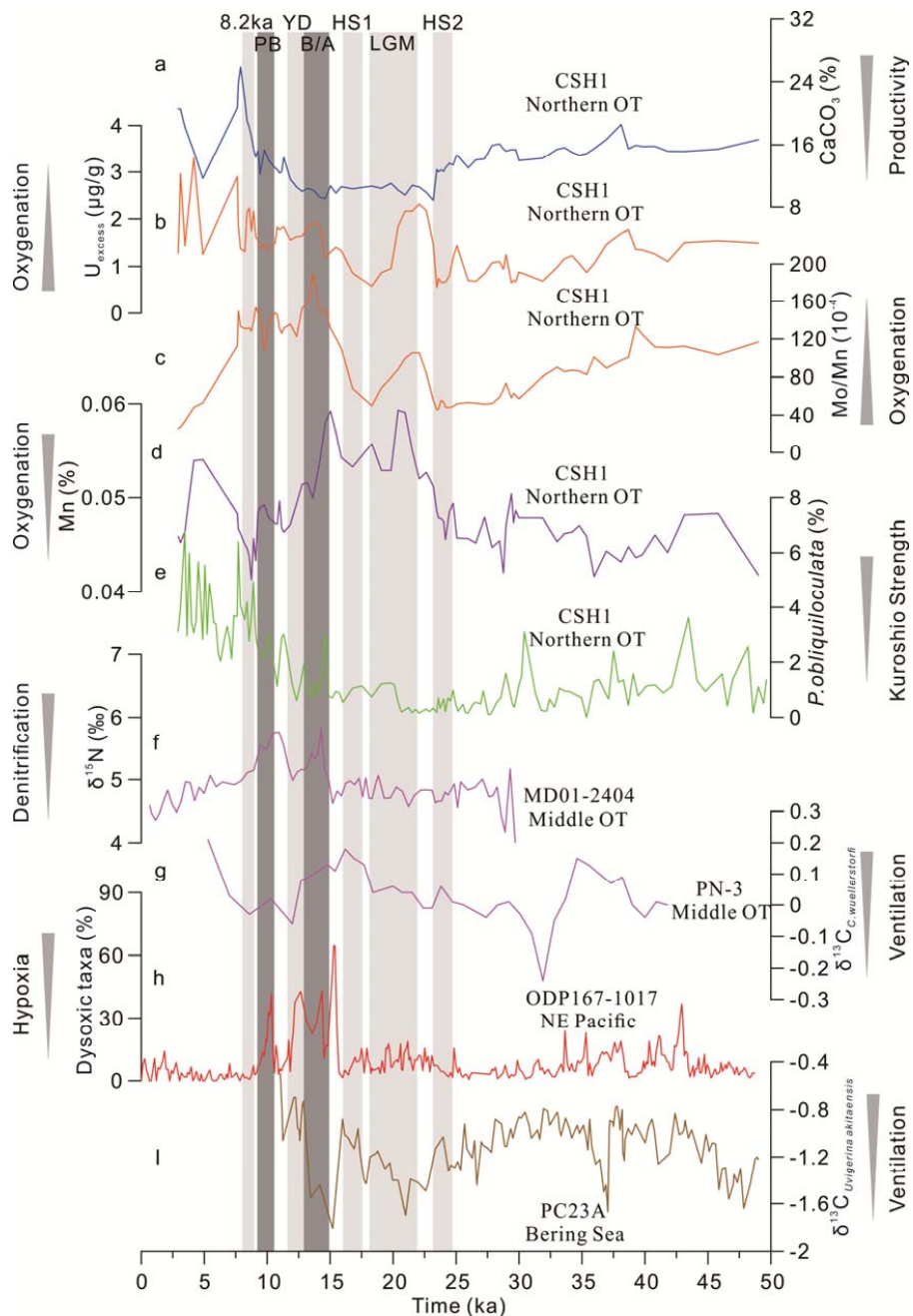


22

23



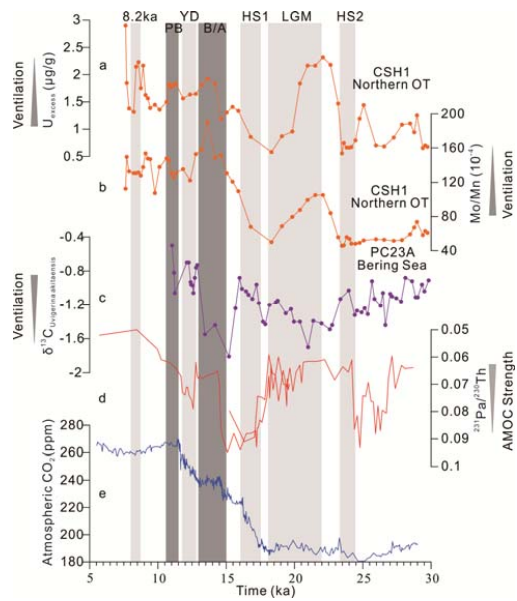
24 Fig.6



25
 26



27 Fig.7



28